NBER WORKING PAPER SERIES

DO ENVIRONMENTAL MARKETS CAUSE ENVIRONMENTAL INJUSTICE? EVIDENCE FROM CALIFORNIA'S CARBON MARKET

Danae Hernandez-Cortes
Kyle C. Meng

Working Paper 27205
http://www.nber.org/papers/w27205

NATIONAL BUREAU OF ECONOMIC RESEARCH
1050 Massachusetts Avenue
Cambridge, MA 02138
May 2020, Revised February 2021

This paper has benefited from comments by Maximilian Auffhammer, Spencer Banzhaf, Youssef Benzarti, Severin Borenstein, Jim Bushnell, Kelly Caylor, Chris Costello, Olivier Deschenes, Meredith Fowlie, Corbett Grainger, Larry Goulder, Kelsey Jack, Arturo Keller, Gary Libecap, Emily Maynard, Andrew Plantinga, David Pellow, Ed Rubin, Jim Salzman, Sam Stevenson, Alisa Tazhitdinova, Chris Tessum, and Paige Weber. We are also grateful for feedback received at various seminars and conferences. Kent Strauss and Vincent Thivierge provided excellent research assistance. Use was made of computational facilities purchased with funds from the National Science Foundation (CNS-1725797) and administered by the Center for Scientific Computing (CSC). The CSC is supported by the California NanoSystems Institute and the Materials Research Science and Engineering Center (MRSEC; NSF DMR 1720256) at UC Santa Barbara. The views expressed herein are those of the authors and do not necessarily reflect the views of the National Bureau of Economic Research.

Do Environmental Markets Cause Environmental Injustice? Evidence from California's Carbon Market

Danae Hernandez-Cortes and Kyle C. Meng

NBER Working Paper No. 27205
May 2020, Revised February 2021
JEL No. H4,I14,Q5,Q51,Q52,Q53,Q54

ABSTRACT

Market-based environmental policies are widely adopted on the basis of allocative efficiency. However, there is growing concern that these market forces could widen existing disparities in pollution exposure between disadvantaged and other communities. Understanding whether such "environmental justice" (EJ) gaps widen or narrow requires estimating effects on pollution emissions and then tracking where that pollution goes. We develop an estimation framework that explicitly embeds a pollution dispersal model to examine how EJ gaps changed following the 2013 introduction of California's green- house gas (GHG) cap-and-trade program, the world's second largest carbon market and the one most subjected to EJ critiques. We find that the program reduced GHG and criteria air pollution emissions. Examining resulting spatial changes in pollution exposure, we find that the program reversed previously widening EJ gaps in PM2:5, PM10, NOx, and SOx, narrowing gaps to 2008 levels by 2017. We demonstrate that using a pollution dispersal model is crucial for the robustness of our results and note that our approach for mapping emissions to exposure is applicable to many environmental policy settings.

Danae Hernandez-Cortes
Department of Economics
University of California, Santa Barbara
Santa Barbara, CA 93106
hernandezcortes@umail.ucsb.edu

Kyle C. Meng
Bren School of Environmental
Science and Management
Department of Economics
University of California, Santa Barbara
4416 Bren Hall
Santa Barbara, CA 93106
and NBER
kmeng@bren.ucsb.edu

1 Introduction

Over the last three decades, policy makers have increasingly relied on market-based environmental policies - such as pollution trading and taxes - to address environmental problems. Expanded use of market-based policies followed each major amendment to the U.S. Clean Air Act since the 1970s (Schmalensee and Stavins, 2019). Widespread adoption has occurred in other environmental domains: today, market-based policies cover 30% of global fisheries (Costello et al., 2016), account for over $36 billion in global ecosystem service payments (Salzman et al., 2018), and govern 20% of global greenhouse gas (GHG) emissions (World Bank Group, 2019).

The central appeal of market-based environmental policies is allocative efficiency. In theory, such policies reduce the total abatement cost of meeting an environmental objective by inducing less abatement from polluters with higher abatement costs (Crocker, 1966; Dales, 1968; Montgomery, 1972). This contrasts with traditional command-and-control regulations, which typically require heterogeneous polluters to adopt uniform abatement actions.

At the same time, the reallocation induced by market-based environmental policies also spatially alters where pollution occurs and thus who are harmed by it. This is of particular concern as a growing "environmental justice" (EJ) literature has documented that communities with lower income, greater minority share, and/or otherwise disadvantaged, are systematically exposed to higher levels of pollution than other communities, a statistic we refer to as the environmental justice gap (or EJ gap).[1] Could the adoption of environmental markets be compounding existing EJ gaps?

Whether a market-based environmental policy widens or narrows the EJ gap depends on the joint spatial distribution of polluting facilities, their abatement costs, and disadvantaged communities. Market-based policies induce relatively less abatement from facilities with steeper marginal abatement cost curves. If these facilities are upwind of disadvantaged communities, such policies will widen an existing EJ gap. Conversely, if these facilities are upwind of non-disadvantaged communities, a market-based policy will narrow the EJ gap (Burtraw et al., 2005).[2] Unfortunately, facility-level marginal abatement cost curves are usually unobserved, making it hard to anticipate the direction of EJ gap effects ex-ante.[3]

[1] EJ gaps across many settings have been shown through case (Bullard, 2000; Bowen, 2002; Ringquist, 2005; Mohai, Pellow and Roberts, 2009; Banzhaf, Ma and Timmins, 2019) and population-level (Tessum et al., 2019; Colmer et al., 2020; Currie, Voorheis and Walker, 2020) studies.

[2] Additionally, for a policy regulating global pollutants like greenhouse gases, the EJ gap effect depends on the extent in which GHG and local pollutants are co-produced.

[3] This observational challenge is not unique to market-based environmental policies. Consider a 2-agent pure exchange economy where agents receive initial endowments. Anticipating whether the welfare gap widens or narrows under the competitive equilibrium compared with autarky requires knowing each agent's preferences.

This difficulty underscores the need for ex-post empirical approaches, for which prior studies of cap-and-trade programs have largely found inconclusive EJ effects (Fowlie, Holland and Mansur, 2012; Grainger and Ruangmas, 2018; Shapiro and Walker, 2021).

This paper estimates the EJ gap consequences of California's greenhouse gas (GHG) cap-and-trade (C&T) program, which since 2013 has created the world's second largest carbon market. This program has also been a focal point of EJ concerns.[4] Because GHG emissions are typically co-produced with local air pollutants, the possibility that the program could widen California's existing EJ gaps in local air pollution has, among other critiques, led to political opposition that temporary paused the program's initial development in 2011 and nearly halted renewal efforts in 2017. However, to date, there has been limited causal evidence on whether the program has indeed widened EJ gaps.

We make two contributions, one empirical and one methodological, in order to establish the EJ gap consequences of California's C&T program. First, we find that the C&T program has lowered GHG and criteria air pollution (i.e., $PM_{2.5}$, PM_{10}, NO_x, and SO_x) emissions. To estimate these effects, we exploit the program's facility-level eligibility rule based on historical emissions and the program's timing to estimate a break in differential emission trends between regulated and unregulated facilities after 2013. This empirical strategy is possible because the emissions-based eligibility threshold for the program is well above the emissions data reporting threshold, allowing us to observe facility-level GHG and criteria air pollution emissions for regulated and unregulated facilities across California, as well as for periods before and after the program's introduction.

These data features are not common across previously studied cap-and-trade programs. For example, facility-level pre-program emissions are not directly observed for the European Union Emissions Trading System (EU-ETS), the world largest carbon market (Martin, Muûls and Wagner, 2016), with researchers having to impute facility emissions using data on fuel inputs and aggregate emissions intensities (Petrick and Wagner, 2014; Colmer et al., 2020). Even when emissions are directly observed, there may not be enough of a difference between program eligibility and data reporting thresholds for there to be sufficient control units within the same jurisdiction. For example, studies of the RECLAIM NO_x C&T program in the Los Angeles region use polluting facilities elsewhere in California as control units, matching treated and control units based on historical emissions levels (Fowlie, Holland and Mansur, 2012). Our approach has the advantage of comparing regulated and unregulated units within the same jurisdiction. However, because treatment is defined according to

[4]Similar EJ concerns have arisen elsewhere. Recent efforts to introduce state-level U.S. climate policies and renew the European Union Emissions Trading System were opposed on EJ grounds (Leber, 2016; Herron, 2019; Transnational Institute, 2013).

historical emissions levels, we cannot expect regulated and unregulated facilities to exhibit similar pre-program emissions levels or even similar pre-program emission trends. Instead, our identifying assumption requires that any existing differential emission pre-trends between regulated and unregulated facilities would have continued after 2013 if not for the C&T program.

We estimate that between 2012-2017, the program reduced emissions annually at a rate of 3-9% across GHG and criteria air pollutants for sample facilities. Demonstrating that California's GHG C&T program has lowered GHG and criteria air pollution emissions is noteworthy by itself. In particular, when an economy-wide C&T program coexists with sector-specific climate regulations, as is the case in California, it is possible that overall GHG reductions are largely, or only, induced by these other regulations, undermining the allocative efficiency argument for using market-based policies (Borenstein et al., 2019). Indeed, because of these "overlapping" regulations, it remains unclear whether the C&T program has contributed to the observed overall decline in California's GHG emissions (Burtraw et al., 2018). We find that it has. We demonstrate that our emissions effects are robust to various model specification and sample restriction choices, concerns about spillover effects between regulated and unregulated facilities, and does not exhibit meaningful heterogeneity according to a facility's average emissions. In a placebo test that systematically imposes trend breaks across sample years, we detect the largest trend break in 2013, the year when the program was actually introduced.

Our second contribution is to develop an empirical approach for determining how policy-driven changes in pollution *emissions* alter the spatial distribution of pollution *exposure*. The canonical framework in economics for evaluating any environmental policy requires knowing the link between a pollution's "source" and its "receptors" (Baumol and Oates, 1988). In practice, however, one rarely knows this mapping. This is particularly true for air pollution: once pollution leaves a smokestack, it is very hard to know where it goes, and therefore who is affected by it. Instead, researchers typically assume a particular mapping between emissions and exposure. For example, it is common to assume that a facility's emissions disperse only within the same geographic unit or within a distance circle around that facility (Banzhaf, Ma and Timmins, 2019). These approaches, however, overlook the complex nature of pollution dispersal which, depending on atmospheric conditions and topography, can disperse pollution in varying directions and distances. Failure to accurately account for pollution dispersal can lead to treatment spillovers that could bias estimates even in otherwise valid quasi-experimental settings (Deschenes and Meng, 2018).

To address this challenge, we explicitly embed pollution dispersal into our estimation framework. We employ an atmospheric dispersal model to convert C&T-driven facility-level

emissions into resulting pollution exposure across all locations in California. This atmospheric dispersal model takes into account topographical features and time-varying atmospheric conditions every four hours within our sample period, a computationally-intensive procedure involving over two million pollution trajectories. We further apply a bootstrap procedure to account for uncertainty in estimated C&T emissions effects. Altogether, our approach extends prior uses of atmospheric dispersal models (Sullivan, 2017; Grainger and Ruangmas, 2018) by combining causal estimates of C&T effects on emissions with a location-specific analysis to examine resulting changes in EJ gaps.

Employing a definition of a "disadvantaged" zip code that serves as a basis for California's EJ policies, we report three EJ gap findings. First, consistent with EJ concerns in the lead up to the C&T program's introduction, we show that not only were there baseline EJ gaps across criteria air pollutants in 2008, but that gaps were widening in the 2008-2012 period before the program. Second, since 2013, EJ gaps have been narrowing because of the C&T program. Third, while EJ gaps have narrowed, they have not been eliminated: by 2017, the C&T program returned EJ gaps roughly to where they were in 2008. We show that our EJ gap results are stable across a variety of robustness checks. In particular, we demonstrate similar EJ gap effects when employing an alternative atmospheric dispersal model that generates secondary pollution exposure. Spatial heterogeneity analysis reveals that post-C&T EJ gaps narrowed the most for disadvantaged zip codes in California's Central Valley, while a few disadvantaged zip codes in Los Angeles County experienced widening EJ gaps.

We demonstrate the importance of modeling pollution dispersal for our results. We show that our EJ gap findings become unstable if instead of modeling pollution dispersal, we were to employ more conventional approaches for assigning pollution emissions to exposure, such as restricting areas of exposure to within a facility's zip code or within distance circles (of varying radii) of a facility. We posit that our approach for embedding a pollution dispersal model within a program evaluation framework has broader applicability. In particular, there is a common need across many environmental policy settings to track how policy-driven changes in pollution emissions alter the spatial distribution of pollution exposure (Greenstone and Gayer, 2009; Graff Zivin and Neidell, 2013; Deschenes and Meng, 2018).

The paper is structured as follows: Section 2 provides a conceptual framework for how a C&T program could widen or narrow an existing EJ gap and offers background on California's GHG C&T program. Section 3 summarizes our data. Section 4 details our empirical approach. Section 5 presents our results. Section 6 provides a concluding discussion.

2 Background

This section discusses how the introduction of a cap-and-trade (C&T) program can either widen or narrow existing pollution exposure gaps between disadvantaged and other communities. We then provide institutional background for California's greenhouse gas (GHG) cap-and-trade program.

2.1 Cap-and-trade and the environmental justice gap

In a textbook C&T program, the regulator establishes a limit (or cap) on total emissions within a jurisdiction by issuing a fixed supply of emission permits. Regulated facilities are then either given, or must purchase, permits to cover their emissions. Permit trading allows the marginal abatement cost (MAC) of emissions to be equalized amongst regulated facilities to the permit price.[5]

The economics literature has emphasized two key consequences of C&T. First, by placing a price on pollution, a C&T program induces polluting facilities to internalize (some of) the social costs of their emissions.[6] Second, by equalizing MACs across facilities, a C&T program allocates emissions by inducing relatively less abatement from facilities with steeper MAC curves and more abatement from facilities with flatter MAC curves. In theory, the resulting allocation of abatement achieves the aggregate emissions cap at the lowest total abatement cost across regulated facilities (Montgomery, 1972).

What is less clear is how the allocative efficiency achieved by a C&T system alters the spatial distribution of pollution exposure. In particular, there is growing concern that the same market forces resulting in allocative efficiency may also be altering the difference in pollution exposure between disadvantaged and other communities. This difference, which we call the "environmental justice gap" (or EJ gap) has been shown to be positive in the many settings (Bullard, 2000; Bowen, 2002; Ringquist, 2005; Mohai, Pellow and Roberts, 2009; Banzhaf, Ma and Timmins, 2019; Tessum et al., 2019; Colmer et al., 2020; Currie, Voorheis and Walker, 2020).

The introduction of C&T can either widen or narrow an existing EJ gap. Figure 1 illustrates this ambiguous effect for a stylized two-facility setting with emissions (e) on the horizontal axis and permit prices (τ) on the vertical axis. The first facility is upwind of a disadvantaged community (DAC) with a marginal abatement curve labeled "DAC" (in orange). The second facility is upwind of a non-disadvantaged community and has a marginal

[5] The modern C&T framework was initially developed by Crocker (1966) and Dale (1968).

[6] Whether social costs are fully internalized depends on if the cap is set at the socially optimal level.

abatement curve labeled "non-DAC" (in gray).[7] To establish an existing positive EJ gap prior to the introduction of C&T, we allow the DAC facility to have larger emissions in the absence of C&T, or when $\tau = 0$. When C&T is introduced, each facility's MAC is equated to the equilibrium permit price $\tau = \tau^*$. What happens to the EJ gap?

In the left panel of Figure 1, the DAC facility has a steeper MAC curve than the non-DAC facility, causing the DAC facility to abate less than the non-DAC facility under C&T. In this case, C&T widens the EJ gap. The right panel of Figure 1 shows an alternative case whereby the DAC facility has a flatter MAC curve than the non-DAC facility. Following C&T, the DAC facility abates more than the non-DAC facility, narrowing the EJ gap.

Thus, in settings with an existing positive EJ gap, whether C&T widens or narrows the EJ gap depends on whether facilities upwind of DAC communities have relatively steeper or flatter MAC curves. Additionally, for a cap-and-trade system regulating a global pollutant such as greenhouse gases, the EJ gap effect depends on the extent in which GHG and local air pollutants are co-produced.

Figure 1: EJ gap under cap-and-trade

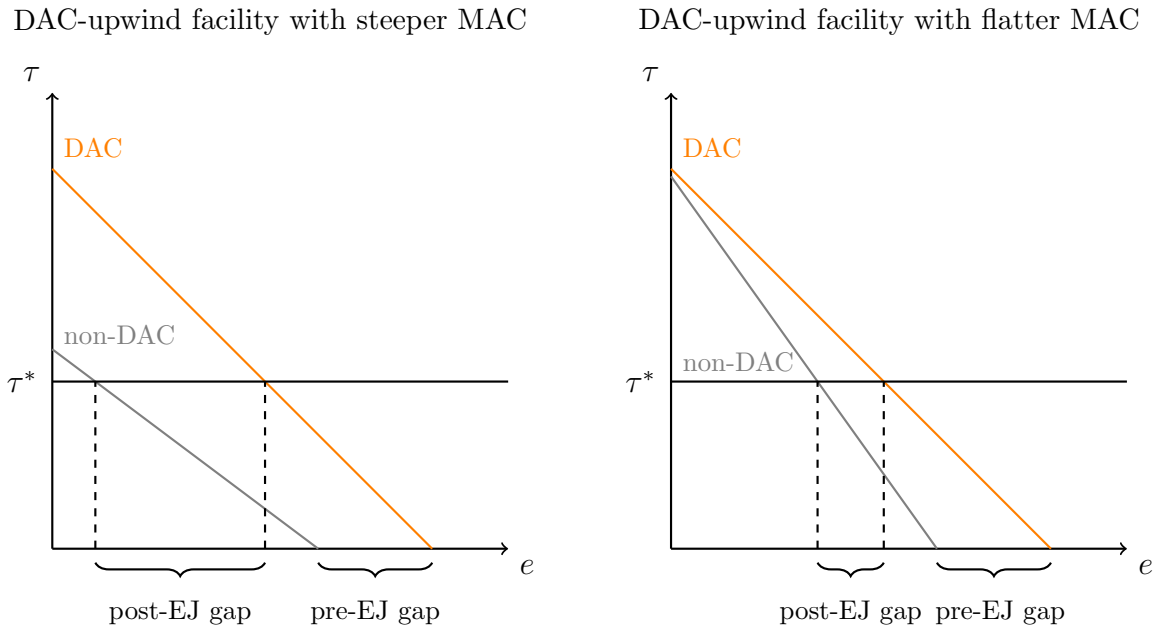

NOTES: Panels illustrate how the introduction of a C&T program can widen or narrow an existing EJ gap in a two facility setting. Horizontal axes indicate emissions. Vertical axes indicate marginal abatement costs, and equivalently the permit price under C&T. The marginal abatement cost curve for facility upwind of a disadvantaged community (labeled DAC) is shown in orange. The marginal abatement cost curve for facility upwind of a non-disadvantaged community (labeled non-DAC) is shown in gray. τ^* indicates the permit price under C&T. In the left panel, the DAC-upwind facility has a relatively steeper MAC curve. In the right panel, the DAC-upwind facility has a relatively flatter MAC curve.

[7] The horizontal axes in Figure 1 indicates emissions rather than abatement in order to illustrate emissions levels prior to C&T when $\tau = 0$.

There are several empirical challenges to resolving this ambiguity. First, facility-level MAC curves are rarely observed, which limits the ability to anticipate EJ gap consequences of proposed C&T programs. Instead, one can empirically estimate EJ gap consequences following the introduction of a C&T program ex-post. To do so, one needs to first obtain causal estimates of the impact of C&T on facility-level emissions, map C&T-driven facility-level emissions onto location-based pollution exposure, and then examine who the resulting exposure is distributed between disadvantaged and non-disadvantaged communities. Section 4 details our procedure for overcoming these challenges.

2.2 California's GHG cap-and-trade program

California's has one of the world's most sophisticated and ambitious climate policies. In 2006, California passed Assembly Bill 32 (AB 32), requiring state-wide GHG emissions to reach 1990 emissions level by 2020. AB 32 was, and remains, the first of its kind: all other climate policies in the U.S. (state or national) regulate specific sectors, whereas AB 32 covers all GHG emission sources in California.

To meet this GHG target, AB 32 established a suite of climate programs. One key program was cap-and-trade, introduced in 2013 and administered by the California Air Resources Board (CARB). The program requires participation by all stationary GHG-emitting facilities producing at least 25,000 metric tons of annual carbon dioxide equivalent emissions, or CO_2e, during any year between 2009-2012.[8] This eligibility criteria covers all sectors that directly emit GHGs from stationary sources and is unique amongst other AB 32 climate programs.[9,10] California's C&T program has since created the world's second largest carbon market by permit value, following the European Union Emissions Trading System (EU-ETS).

In 2016, California met AB 32's 2020 GHG target four years early. That same year, the state extended its GHG target to 40% below 1990 levels by 2030. This was shortly followed by a 2030 extension of the C&T program. However, critical questions remain regarding the performance and consequences of the C&T program.

First, it remains unclear whether the C&T program has caused lower GHG emissions. In particular, when a C&T program coexists with other climate programs, as is the case under AB 32, an overall GHG emissions cap can be met with little or no abatement induced by

[8] Greenhouse gases covered by the program were CO_2, CH_4, N_2O, HFCs, PFCs, SF6, NF3 and other fluorinated GHGs.

[9] The 2013 timing of the C&T program is also unique. Most other AB 32 climate programs were introduced earlier.

[10] It should be noted that the GHG C&T program does not directly regulate emissions of local criteria air pollutants. Any changes in the spatial distribution of local air pollution exposure due to the program is thus driven by the program's reallocation of GHG emissions and the co-production of local air pollutants with GHGs.

the C&T program if most or all abatement is dictated by these complementary programs.[11] Indeed, an ex-ante analysis of California's GHG C&T program demonstrate a potentially large role played by such complementary programs on overall GHG abatement (Borenstein et al., 2019).[12] Second, even if the C&T program had lowered GHG and related local air pollution emissions, it remains to be established whether the resulting distribution of air pollution exposure has caused existing pollution exposure gaps between disadvantaged and other communities in California to widen or narrow.

3 Data

Our analysis involves two primary datasets: 1) emissions of criteria air pollutants at the facility-by-year level and 2) an indicator of whether a zip code is assigned to be "disadvantaged" according to a policy-relevent definition defined by California.

Air pollution emissions We obtain 2008-2017 facility-level annual emissions of GHG (in CO2e), $PM_{2.5}$, PM_{10}, NO_x, and SO_x from CARB's Pollution Mapping Tool.[13] Stationary facilities with annual emissions past a certain threshold must report emissions to CARB. For $PM_{2.5}$, PM_{10}, NO_x, and SO_x, the reporting threshold is 10 metric tons per year. For GHGs, the reporting threshold is 10,000 metric tons of CO_2e. Because this reporting threshold is below the C&T program's GHG eligibility threshold, we observe GHG as well as criteria air pollutions emissions for both C&T-regulated and non-regulated stationary facilities, before and after the introduction of the C&T program.[14]

Several additional facility-level variables serve as inputs for the atmospheric dispersal model. CARB provides facility latitude and longitude as well as pollution-specific stack heights for a subset of facilities. For other facilities, we impute missing pollution-specific stack heights using sector averages constructed from non-missing observations.

Zip code definition of a disadvantaged community There is no established definition of a "disadvantaged" community. Previous papers in other settings use a location's median

[11] Prominent complementary programs to C&T under AB 32 include a Renewable Portfolio Standard for electricity generation and a Low Carbon Fuel Standard for refineries.

[12] Furthermore, even a positive GHG permit price does not ensure that the C&T program caused GHG emissions to fall. Suppose, for example that there was some form of restriction on GHG emissions prior to the C&T program leading to a pre-program positive shadow price on GHG abatement. A C&T program with an overall cap set equal to total emissions under the prior restriction would generate a positive permit price despite no change in overall GHG emissions.

[13] Available here: https://ww3.arb.ca.gov/ei/tools/pollution_map/

[14] Details on CARB's reporting requirements can be found here: https://ww3.arb.ca.gov/ei/tools/pollution_map/doc/caveats%20document12_22_2017.pdf

income or minority share of population as proxy measures (Fowlie, Holland and Mansur, 2012; Grainger and Ruangmas, 2018; Mansur and Sheriff, 2019). For our setting, we select a policy-relevant definition of a "disadvantaged" community. Senate Bill 535 (SB 535), passed in 2012, requires a portion of the revenue from the auction of C&T permits to be directed towards benefiting disadvantaged communities. We employ this definition because it is the basis for which zip codes receive government funds to offset environmental justice concerns. SB 535 formally defines a "disadvantaged community" using CalEnviroScreen, a scoring system based on multiple indicators developed by the California Environmental Protection Agency. Specifically, a zip code is considered disadvantaged if it contains all or part of a census tract with a CalEnviroScreen score above the top 25th percentile. Zip codes designated as disadvantaged are shaded in dark blue in Figure 2a. Importantly, pre-2013 data was used in constructing CalEnviroScreen, which mitigates the concern that cap-and-trade may have affected zip code designation. We further augment our zip code level data with average 2008-2012 population obtained from the U.S. Census Bureau.

4 Empirical approach

Our analysis proceeds along three steps. First, we use facility-by-year-level data to estimate how the GHG C&T program altered GHG, $PM_{2.5}$, PM_{10}, NO_x, and SO_x emissions. Second, we feed C&T-driven $PM_{2.5}$, PM_{10}, NO_x, and SO_x emissions predicted from the first step into an atmospheric dispersal model to generate zip code-by-year-level exposure of these pollutants due to the program. Finally, we examine whether the C&T program changed the exposure gap for these pollutants between disadvantaged and other communities following its 2013 introduction.

Step 1: Estimating C&T effects on emissions We exploit the facility-level eligibility criteria based on pre-program GHG emissions and the 2013 timing of the C&T program to identify its effects on GHG, $PM_{2.5}$, PM_{10}, NO_x, and SO_x facility-level emissions during 2008-2017. Because the program's eligibility criteria is based on pre-C&T GHG emissions, we expect regulated and unregulated facilities to differ in pre-program emissions levels and perhaps also in pre-program emission trends. Our empirical test therefore examines whether differential emission trends exhibit a break after 2013. For this test to have a causal interpretation, our identifying assumption requires that any existing differential emission pre-trends to have continued if not for the introduction of the C&T program.[15]

[15] Note that because there is no overlap in pre-program GHG emissions for regulated and unregulated facilities, we are unable to implement a matching estimator that matches on pre-program emissions, as is

Specifically, let j index facilities. $C_j \in \{0, 1\}$ is GHG C&T regulatory status with $C_j = 1$ indicating facility j is regulated.[16] For facility j in year t, Y_{jt}^p is annual emissions of pollutant $p \in \{GHG, PM_{2.5}, PM_{10}, NO_x, SO_x\}$. Because emissions exhibit a skewed distribution and contain zero values, we apply an inverse hyperbolic sine transformation, which like a log transformation lends a percentage effect interpretation, but with the added advantage of retaining zero-valued observations (Bellemare and Wichman, 2020). To examine differential emission trends driven by the C&T program, we estimate the following specification:

$$asinh(Y_{jt}^p) = \kappa_1^p[C_j \times t] + \kappa_2^p[C_j \times \mathbf{1}(t \geq 2013) \times t] + \phi_j^p + \gamma_t^p + \mu_{jt}^p \quad (1)$$

Facility-specific dummy variables ϕ_j^p removes time-invariant determinants of pollution p for facility j. Year-specific dummy variables γ_t^p remove common determinants of emissions affecting all sample facilities in year t, such as California-wide economic conditions.

κ_1^p captures the differential emission pre-trend for pollutant p between facilities that would and would not eventually be regulated by the C&T program during 2008-2012, reported in annual percentage point changes. κ_2^p is the change, or break, in the differential emission trend after the program's introduction during 2013-2017. μ_{jt}^p is clustered at the county-level to allow for arbitrary forms of heteroskedasticity and serial correlation within a county.

We employ two sample restrictions to strengthen identification of trend break effects in equation (1). First, despite the C&T program's unique eligibility criteria and timing, the presence of other major climate programs under AB 32, such as the Renewable Portfolio Standard for electricity generators and the Low Carbon Fuel Standard for refineries, may confound C&T effects for these facilities. We remove electricity generators and refineries from our sample to avoid this possibility.[17] Second, to ensure better comparability between treated and control facilities, we restrict our sample to facilities with sample average annual GHG emissions below the 75th percentile.[18] As a robustness check, we consider smaller and larger cutoff percentiles. Our benchmark sample contains 106 regulated and 227 unregulated facilities. Each regulated facility is shown as a black dot in Figure 2a. Table S1 shows how

done in Fowlie, Holland and Mansur (2012) and Martin, Muûls and Wagner (2016). Implementing such a matching approach would require emissions data from facilities outside of California. That comparison, however, may be confounded by systematic unobserved differences between California and non-California facilities.

[16] All but 39 facilities that emit local air pollution found in CARB's Pollution Mapping Tool have time-invariant GHG C&T regulatory status between 2008-2017. All 39 facilities with time-varying statuses switch status only in 2017. Because we do not know if these switches are due to actual changes in regulatory status or coding errors, we drop these 39 facilities from our sample such that all sample facilities have time-invariant regulatory status.

[17] This restriction also addresses concerns about the the 2013 closure of the San Onofre Nuclear Generating Station, a power plant in southern California (Davis and Hausman, 2016).

[18] The 75th percentile corresponds to average annual emissions of 62,770 metric tons of CO_2e.

these facilities are distributed across sectors.

To construct facility-by-year emissions driven by the C&T program (relative to California-wide determinants of pollution), we apply a hyperbolic sine transformation to the first two terms of equation (1) and the estimated facility-level fixed effect.[19] Because facilities differ by average emission levels, the inclusion of facility-level fixed effects allows us to generate heterogeneous C&T-driven pollution abatement across regulated facilities despite estimating a common percentage effect.[20] This implicitly assumes that larger emitting facilities abate more under C&T. To examine this assumption, in a robustness check, we also estimate variants of equation (1) that allow the post-C&T trend break to vary as linear and quadratic functions of facility-level average annual emissions.

Step 2: Modeling pollution dispersal Our second step determines how C&T-driven criteria air pollution disperses spatially across California. The standard approach is for the researcher to prescribe the set of locations exposed to emissions from a particular source, either by assuming emissions only affects areas in the same administrative unit of the source or within a radially uniform distance from the source. For example, one may assume emissions from a facility in Los Angeles County only affect Los Angeles County or areas within a certain radial distance of that facility. Actual areas affected by pollution from that facility, however, may not conform to these assumptions and instead may vary depending on topography or time-varying meteorological conditions. To fully capture the complexity of pollution dispersal, we turn to modeling it explicitly.

We feed predicted facility-by-year $PM_{2.5}$, PM_{10}, NO_x, and SO_x emissions from step 1, together with the location and stack height of each facility, into the Hybrid Single Particle Lagrangian Integrated Trajectory Model (HYSPLIT), an atmospheric dispersal model developed by the U.S. National Oceanographic and Atmospheric Administration (NOAA) with meteorological conditions from NOAA's 40-km resolution North American Model Data Assimilation System (NAMDAS) (Draxler and Hess, 1998). An emerging literature uses HYSPLIT to convert pollution emissions to exposure (Grainger and Ruangmas, 2018; Henneman, Mickley and Zigler, 2019; Casey et al., 2020).

[19] Specifically, C&T-driven emissions is:

$$\widehat{Y}^p_{jt} = sinh\left(\widehat{\kappa}^p_1[C_j \times t] + \widehat{\kappa}^p_2[C_j \times \mathbf{1}(t \geq 2013) \times t] + \widehat{\phi}^p_j\right) * e^{(RMSE)^2/2)}$$

where hat notation indicates estimated parameters and RMSE is the root mean squared error from equation (1). In theory, the hyperbolic sine transformation can generate negative emission values. In practice, our benchmark model predicts negative emissions for 1%, 1%, 0.2%, and 0.3% of sample observations for $PM_{2.5}$, PM_{10}, NO_x, and SO_x, respectively. We replace these negative values with zeros.

[20] For example, a 10% abatement effect implies 10 tons of abatement for a facility with 100 tons of average annual emissions and 5 tons of abatement for a facility with 50 tons of average annual emissions.

We choose HYSPLIT because it provides a middle-of-the-road approach for our application, balancing atmospheric realism with computational tractability. HYSPLIT is less computationally intensive than chemical dispersal models such as WRF-Chem, but at the cost of not incorporating atmospheric chemistry which is important for modeling secondary pollutant formation. At the same time, HYSPLIT is more reliable for modeling pollution dispersal beyond distances of 50 kilometers, which less computationally-intensive Gaussian-plume models like AERMOD or APEEP do poorly (EPA, 2015).

We note several features of our HYSPLIT implementation. First, to account for high-frequency variation in meteorological conditions, we run forward particle trajectories at four hour intervals, implicitly assuming that annual emissions are distributed uniformly within the year. Each trajectory runs for 24 hours, a duration long enough to ensure most emitted particles leave California. Second, because HYSPLIT does not explicitly account for particle decay, we apply half-life parameters from the atmospheric chemistry literature set at 24 hours for $PM_{2.5}$ and PM_{10}(U.S. EPA, 2018), 3.8 hours for NO_x (Liu et al., 2016), and 13 hours for SO_x (Lee et al., 2011). Third, we assume that a particle no longer contributes to surface pollution concentrations once it exits the planetary boundary layer, beyond which there is far less turbulent mixing. We conservatively set the boundary layer height at 1 km above the surface, which is about double the typical height for California (Rahn and Mitchell, 2016). As a robustness check, we also consider boundary layer heights of 0.5 and 2 km. As an illustration of pollution dispersal modeled by HYSPLIT, Figure 2b shows the trajectories of pollution emitted by a regulated facility in Los Angeles during 2016. In total, we compute over 2 million particle trajectories from the roughly one hundred regulated facilities in our sample during the 2008-2017 period. This procedure takes about 24 hours to complete with over one thousand facility-by-year parallelized nodes on a high-performance computing cluster.

To obtain zip code-by-year pollution exposure (in $\mu g/m^3$) due to C&T-driven emissions, we sum across HYSPLIT trajectories for each zip code and year and divide by the volume of the atmosphere between a zip code's surface and the boundary layer. We further divide by 365 to obtain an average daily measure of HYSPLIT-generated pollution exposure. Figure 2c show our benchmark HYSPLIT-generated daily exposure (in $\mu g/m^3/day$) for each zip code, averaged across 2008-2017 for $PM_{2.5}$. Figure S3 similarly shows average 2008-2017 zip-code exposure for PM_{10}, NO_x, and SO_x.[21]

Lastly, as noted, a major limitation with HYSPLIT is that it does not model secondary

[21]Figure 2, Figure S3, and Table S6 show that criteria air pollution from GHG C&T-regulated facilities disperses across all of California and not just zip codes designated as disadvantaged. This implies that any change in average pollution exposure between disadvantaged and other zip codes occurs because the GHG C&T program alters the differential exposure between disadvantaged and other zip codes.

Figure 2: Modeling air pollution exposure driven by the cap-and-trade program

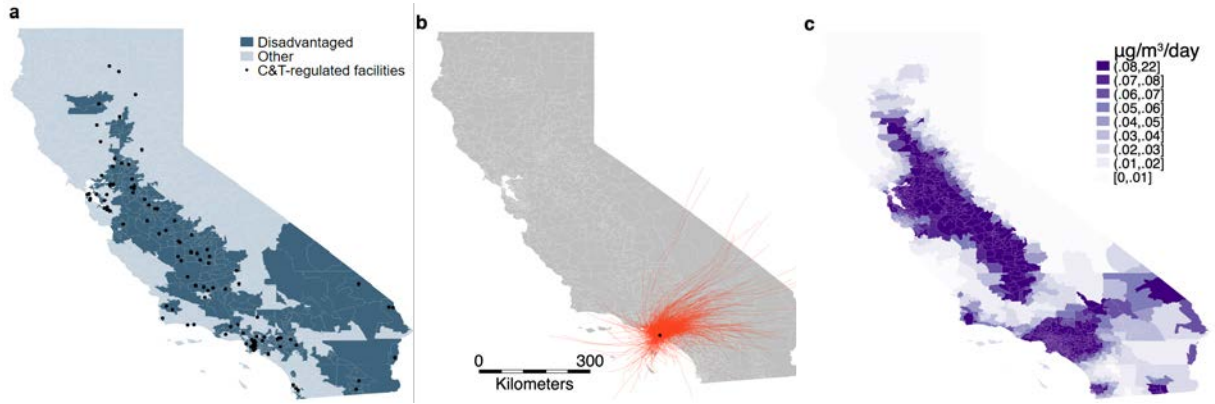

NOTES: Panels illustrates how facility-level emissions is converted to zip code-level pollution exposure using an atmospheric dispersal model. Shading in panel (a) shows California zip codes that are designated as disadvantaged (dark blue) and zip codes that are not (light blue) according to California policy. Black dots show sample facilities regulated by California's GHG C&T program. Panel (b) shows HYSPLIT-generated particle trajectories every 4-hours from a regulated facility during 2016. Panel (c) shows zip code-level average daily $PM_{2.5}$ exposure (in $\mu g/m^3$/day) during 2008-2017 driven by facilities regulated by the C&T program as modeled by HYSPLIT.

pollution formation. To see if secondary $PM_{2.5}$ exposure exhibits a different spatial pattern than primary $PM_{2.5}$ exposure, in a robustness check, we replace HYSPLIT with InMAP, a reduced-complexity dispersal model based on the WRF-Chem model which generates secondary pollutants (Tessum, Hill and Marshall, 2017).

Step 3: Estimating C&T-driven change in EJ gap trends In our third step, we examine whether the C&T program altered the difference in pollution exposure between disadvantaged and other communities, or the EJ gap. Let $D_i \in \{0, 1\}$ denote disadvantaged status, with $D_i = 1$ indicating that zip code i contains all or part of a "Disadvantaged Community Census Tract," as defined by Senate Bill 535. For zip code i in year t, we take C&T-driven pollution exposure from HYSPLIT, E^p_{it} for criteria air pollutant $p \in \{PM_{2.5}, PM_{10}, NO_x, SO_x\}$, and estimate the following specification:

$$E^p_{it} = \beta^p_1[D_i \times t] + \beta^p_2[D_i \times \mathbf{1}(t \geq 2013) \times t] + \psi^p_i + \delta^p_t + \epsilon^p_{it} \tag{2}$$

where ψ^p_i are zip code-specific dummies and δ^p_t are year-specific dummies. β^p_1, or the pre-C&T EJ gap trend, captures the linear trend in the EJ gap (from facilities that would eventually be regulated by the C&T program) during 2008-2012, before the program was introduced. A positive trend (i.e., $\beta^p_1 > 0$) would indicate that the EJ gap was widening prior to the C&T program. Our main parameter of interest is β^p_2, which captures the change in the EJ gap trend after the program's introduction, or the post-C&T EJ gap trend break. Conditional

on $\beta_1^p > 0$, $\beta_2^p < 0$ implies that the introduction of the C&T program slowed the previous positive EJ gap trend. We consider two additional trend break statistics. The first statistic asks whether the post C&T EJ gap trend break is sufficiently large such that the EJ gap has actually narrowed in level terms after the C&T program. This would be captured by $\beta_1^p + \beta_2^p$, or the post-C&T EJ gap trend, with $\beta_1^p + \beta_2^p < 0$ indicating that the EJ gap is narrowing.[22] A second statistic examines the relative degree in which C&T program has slowed the prior EJ gap trend. Specifically, $\frac{\beta_2^p}{\beta_1^p} * 100 = (\frac{(\beta_1^p + \beta_2^p) - \beta_1^p}{\beta_1^p}) * 100$ captures the percentage change in the EJ gap trend following the introduction of the C&T program.

C&T-driven pollution exposure, E_{it}^p, the outcome variable in equation (2), is predicted C&T-driven emissions from equation (1) via HYSPLIT. As a consequence, ϵ_{it}^p, the error term in equation (2), does not account for statistical uncertainty in C&T emission effects from equation (1). Instead, ϵ_{it}^p may capture residuals that arise when estimating an average EJ effect in the presence of heterogeneous EJ effects. To address related concerns over inference, we conduct two standard error adjustments. First, we cluster ϵ_{it} at the county level to allow for arbitrary forms of heteroskedasticity and serial correlation when heterogeneous treatment effects are not independent and identically distributed. Second, to incorporate statistical uncertainty in predicted C&T-driven emissions from equation (1), we conduct a bootstrap procedure drawing multiple vectors of C&T-driven emissions from the estimated empirical distributions of κ_1^p and κ_2^p, which are then fed into steps 2 and 3. In practice, we implement 250 bootstrap draws to generate a component of the standard error for β_1^p and β_2^p that accounts for statistical uncertainty in equation (1). We add this component to the standard error from directly estimating equation (2) when reporting uncertainty for β_1^p and β_2^p. Figure S4 plots the empirical distribution of β_1^p and β_2^p across bootstrapped draws.[23] Appendix A.1 provides more details on this bootstrap procedure.

To estimate an average pollution exposure effect across individuals in California, we weight each zip code-by-year observation in equation (2) by average zip code population during 2008-2012, the period prior to the program.

Before turning to our results, we note that our approach is part of a broader effort across natural and social science disciplines to use pollution dispersal modeling to map pol-

[22] Observe that while $\beta_2^p < 0$ alone implies that the C&T program resulted in EJ gap benefits by slowing the growth in the EJ gap, it does not necessarily imply that this post-trend break effect is strong enough to offset the magnitude of the pre-trend such that EJ gap is narrowing in absolute terms following the program. For that to occur, one needs $\beta_2^p < -\beta_1^p$, or $\beta_1^p + \beta_2^p < 0$.

[23] As with prior literature, we omit uncertainty associated with atmospheric dispersal, or the mapping between facility-level emissions and zip code-level exposure. One possibility involves resampling meteorological conditions in HYSPLIT via a bootstrapping algorithm. Given that our use of HYSPLIT takes 24 hours, overlaying such an approach to the existing 3-step procedure is currently unrealistic under available computational resources.

lution emissions to exposure. Studies in this literature can be broadly classified into two classes. The first group of studies conduct location-level analyses after feeding emissions into a dispersal model but do not explicitly estimate the effects of environmental policies (Ash and Fetter, 2004; Morello-Frosch and Jesdale, 2006; Sullivan, 2017; Cummiskey et al., 2019; Henneman, Mickley and Zigler, 2019; Kim et al., 2020). As such, these studies do not examine policy-driven changes in pollution exposure. A second group of studies estimate whether a policy's effect on facility-level emissions varies with the demographic characteristics of downwind households, as determined by the pollution dispersal model (Grainger and Ruangmas, 2018; Mansur and Sheriff, 2019). However, in these studies it is not obvious how facility-level effects convert to location-specific changes in pollution exposure. Instead, one must explicitly conduct a location-level analysis using pollution exposure arising from policy-driven emissions, as is done with our approach.

5 Results

This section presents our results. Section 5.1 shows the effect of the GHG C&T program on differential emission trends between regulated and unregulated facilities. Section 5.2 examines how these C&T-driven emissions altered trends in the pollution exposure gap between disadvantaged and other communities across California.

5.1 Cap-and-trade effects on emissions

Main results Table 1 reports the pre-C&T differential emissions trend (i.e., κ_1^p from equation (1)) and the post-C&T differential emissions trend break (i.e., κ_2^p from equation (1)) for GHG and criteria air pollutants. Column 1 shows a statistically significant trend break in GHG emissions, indicating that the C&T program led to a reduction in GHG emissions. Prior to the program, the gap in GHG emissions between regulated and unregulated facilities increased at an annual rate of 19 percentage points. Following the introduction of the program, this trend slowed by 30 percentage points such that the gap in GHG emissions actually falls at an annual rate of 11 percentage points between 2012-2017. For criteria air pollutants, columns 2-4 show that there was also a statistically significant, negative emissions trend break following the 2013 introduction of the program for $PM_{2.5}$, PM_{10}, NO_x. For SO_x, the trend break is negative but not statistically significant. Given uncertainty in SO_x emission effects, all subsequent SO_x results should be interpreted with caution.

We predict C&T-driven emissions using estimates in Table 1 together with facility-level fixed effects. This generates heterogeneous facility-level C&T-driven abatement between

2012-2017, or $\widehat{Y}^p_{j,2017} - \widehat{Y}^p_{j,2012}$ as defined in footnote 19, and shown in Figure S2 for GHG, $PM_{2.5}$, PM_{10}, NO_x, and SO_x. Averaged across sample facilities, between 2012 and 2017, the C&T program reduced emissions annually at a rate of 9%, 5%, 4%, 3%, and 9% for GHG, $PM_{2.5}$, PM_{10}, NO_x, and SO_x, respectively.[24,25]

Table 1: Trend break in emissions

	Outcome is (asinh) emissions				
	(1) GHG	(2) $PM_{2.5}$	(3) PM_{10}	(4) NO_x	(5) SO_x
κ_1^p	0.187	0.058	0.083	0.075	0.006
	(0.052)	(0.043)	(0.033)	(0.039)	(0.035)
	[0.001]	[0.183]	[0.016]	[0.061]	[0.875]
κ_2^p	-0.297	-0.097	-0.117	-0.104	-0.037
	(0.077)	(0.048)	(0.039)	(0.050)	(0.043)
	[0.000]	[0.053]	[0.005]	[0.042]	[0.393]
$\kappa_1^p + \kappa_2^p$	-0.111	-0.039	-0.034	-0.029	-0.031
	(0.036)	(0.018)	(0.018)	(0.019)	(0.019)
	[0.004]	[0.039]	[0.068]	[0.138]	[0.108]
Facilities	316	302	302	303	303
Counties	41	40	40	40	40
Observations	2,054	1,968	1,968	1,970	1,965

NOTES: Estimates of pre-C&T differential emissions trend (i.e., κ_1^p from equation (1)) and post-C&T differential emissions trend break (i.e., κ_2^p from equation (1)) for GHG, $PM_{2.5}$, PM_{10}, NO_x, and SO_x across columns. All models include facility-specific and year-specific dummy variables. Standard errors clustered at the county-level in parentheses, p-value in brackets.

Robustness checks We subject these emission effects to several robustness checks. First, Figure S1 considers placebo program start years, plotting κ_2^p for GHG, $PM_{2.5}$, PM_{10}, NO_x,

[24] This is calculated by averaging $(\frac{\widehat{Y}^p_{j,2017} - \widehat{Y}^p_{j,2012}}{\widehat{Y}^p_{j,2012}})/5$, as defined in footnote 19, across regulated sample facilities for each pollutant p.

[25] GHG permit prices for California C&T program has largely hovered above the program's price floor since its inception. We observe detecting emissions abatement from sectors directly regulated by only the C&T program is consistent with permit prices at the price floor when other C&T-covered sectors are further regulated by complementary climate programs, as in the case in California with electricity generators under the Renewable Portfolio Standard and refineries under the Low Carbon Fuel Standard. When such complementary programs bind, aggregate demand for GHG permits fall, causing permit prices to hit the price floor. However, provided that abatement driven by complementary policies are insufficient to meet the GHG cap, the C&T program will still induce abatement from sectors that are regulated only by the C&T program.

and SO_x emissions from variants of equation (1) that impose alternative years for the start of the C&T program across 2009-2016. With the exception of the SO_x models, we detect the strongest trend break coefficient when we assign the treatment year to its actual occurrence in 2013. Second, Table S2 varies the cutoff rule we use on sample average annual GHG emissions when restricting our facility sample. We detect similar trend breaks when we change our benchmark 75th percentile cutoff to the 70th or 80th percentiles.[26]

Third, our predicted C&T-driven emissions which includes facility fixed effects from equation (1), implicitly assumes more pollution abatement from facilities that emit more on average. To examine whether this assumption is reasonable, column 2 of Table S3 reports a variant of equation (1) that further includes an interaction between the trend break term and a linear function of facility-level average emissions. A positive interaction coefficient would imply that larger emitting facilities are abating less, contradicting our assumption. With the exception of GHG emissions for which the linear interaction term is positive but of very small magnitude, the average emissions interaction term for every criteria air pollution is negative. This suggests that our benchmark model, which estimates an average trend break coefficient across facilities (regardless of size) is understating the degree in which facilities that emit more on average are also abating more under C&T. To examine how much, as a robustness check we feed predicted emissions from column 2 of Table S3 into steps 2 and 3 to examine resulting EJ gap effects. Column 3 of Table S3 shows that heterogeneity by average emissions does not exhibit nonlinearity, as indicated by statistically imprecise quadratic interaction terms.

Finally, there may be a Stable Unit Treatment Value Assumption (SUTVA) as pollution may shift from a regulated to unregulated facilities following the introduction of C&T. If so, the resulting increase in unregulated facility emissions may lead to more negative estimates of the trend break parameter κ_2^p. Following Fowlie, Holland and Mansur (2012), we consider two robustness checks in Table S4 to examine this possibility, both of which restrict attention to subsamples of unregulated facilities for which pollution reallocation is harder to undertake.

In the first test, we observe that a facility located in a county under U.S. Clean Air Act nonattainment for a particular pollutant is largely unable to increase pollution levels. This idea is implemented in column 2, which restricts the sample of unregulated facilities to those located in nonattainment counties for that pollutant under the Clean Air Act.[27] Our second

[26]The 70th and 80th percentiles for sample average annual GHG emissions corresponds to 48,834 and 82,173 tons of CO_2e, respectively.

[27]In Table S4, column 2 does not apply to GHG emissions because it is not a criteria pollutant regulated under the Clean Air Act. For SO_x, there are no counties in nonattainment during our sample period. For NO_x, because there were not enough counties under NO_2 nonattainment to construct a control group, we follow Fowlie, Holland and Mansur (2012) by looking at nonattainment under Clean Air Act's one-hour ozone standard as NO_x is a precursor pollutant to ozone.

test notes that firms with multiple facilities can more readily reallocate pollution across their facilities. In column 3, we restrict the control group of unregulated facilities to those whose parent company only operates a single plant.[28] If treatment spillovers were present, the trend break coefficient κ_2^p should be of smaller magnitude in columns 2 and 3 than in our benchmark estimate, shown in column 1. This is not the case.

5.2 Cap-and-trade effects on EJ gaps

Validating pollution dispersal modeling We first consider two sensibility checks for our measure of C&T-driven pollution exposure via HYSPLIT before turning to our main EJ gap results. First, we examine whether HYSPLIT-generated criteria air pollution exposure correlates with monitored ambient air pollution. Specifically, we match zip code-level HYSPLIT-generated pollution exposure averaged over 2008-2017 to the average ambient pollution of that zip code as recorded by pollution monitors averaged over the same period, obtained from the U.S. Environmental Protection Agency.[29] Note that a perfect fit between these two variables is not expected as ambient pollution at any location is composed of emissions originating from many more sources (i.e., stationary and non-stationary, within and beyond California) than our subset of stationary sources regulated by California's GHG C&T program. However, a positive correlation between the two pollution exposure measures would provide reassurance that HYSPLIT-generated pollution exposure from C&T regulated facilities is being detected by ambient pollution monitors. The positive correlations shown in Table S5 indicate that is indeed the case.[30]

Next, we examine the EJ gap in 2008 driven by facilities that would eventually be regulated by the C&T program. Prior work has documented strong baseline EJ gaps in California (Cushing et al., 2018). Indeed, this baseline EJ gap informed initial EJ concerns regarding California's C&T program. Table S6 shows that steps 1 and 2 of our approach reproduces EJ gaps in 2008. Disadvantaged communities experienced higher levels of $PM_{2.5}$, PM_{10}, NO_x, and SO_x exposure in 2008 than other communities on average due to emissions from facilities that would eventually be regulated by the C&T program.

[28] We link each facility from CARB with its parent company as indicated by the EPA. We employ a fuzzy string matching algorithm as facility names are not standardized across the two datasets.

[29] Available here: https://www.arcgis.com/home/item.html?id=8d2012a2016e484dafaac0451f9aea24

[30] We are interested in modeling where C&T-driven pollution is dispersed. As such, we do not directly use ambient pollution data (either from ground-based monitoring stations or remotely-sensed satellites) in our analysis as it is often difficult to determine which component of any location's ambient pollution originates from C&T-regulated facilities. Such "backwards" atmospheric modeling often yield indeterminate results.

Main results We now turn to our main results examining the time evolution of EJ gaps between 2008-2017. They are shown in Table 2 and Figure 3. Across $PM_{2.5}$, PM_{10}, NO_x, and SO_x, the EJ gap widens during 2008-2012, the period prior to the C&T program, as indicated by the positive pre-C&T EJ gap trend (i.e., β_1^p from equation (2)). Following 2013, the EJ gap trend falls: the post-C&T EJ gap trend break (i.e., β_2^p from equation (2)) is negative and statistically significant. This drop in the EJ gap trend is sufficiently large such that the EJ gap is actually narrowing following C&T, as indicated by the negative post-C&T EJ gap trend across pollutants (i.e., $\beta_1^p + \beta_2^p$). In percentage terms (i.e., $\frac{\beta_2^p}{\beta_1^p} * 100$), the EJ gap trend fell between 140-270% across pollutants after the program's introduction. Figure 3 plots this trend break as well as annual EJ gap coefficients from a more flexible version of equation (1) using year-specific EJ gap coefficients.[31] Figure 3 also highlights that while the C&T program has led EJ gaps to narrow since 2012, it has not eliminated them. By 2017, EJ gaps are roughly at 2008 levels across pollutants.

Spatial heterogeneity Estimates from equation (2) shown in Table 2 and Figure 3 examine the time evolution of EJ gaps averaged across disadvantaged and other zip codes. Additionally, one may be interested in how EJ gap effects vary spatially, particularly given the localized nature of EJ concerns. To examine spatial heterogeneity in trend break effects across disadvantaged zip codes, we estimate a variant of equation (2) allowing zip code-specific post-C&T EJ gap trend break coefficients.[32] Figure 4 shows the percentage change in the EJ gap trend following the introduction of C&T for each disadvantaged zip code for $PM_{2.5}$, PM_{10}, NO_x, and SO_x. Across pollutants, post-C&T EJ gaps narrowed the most for disadvantaged zip codes in California's Central Valley. For $PM_{2.5}$, PM_{10}, and NO_x, Figure 4 also shows a cluster of zip codes in Los Angeles County that experienced widening post-C&T EJ gaps. Figure S5 shows histograms for the distribution of percentage changes in EJ gap trends across disadvantaged zip codes.

[31] Specifically, the annual coefficients in Figure 3 are β_τ^p from

$$E_{it}^p = \sum_{\substack{2008 \leq \tau \leq 2017 \\ \tau \neq 2012}} \beta_\tau^p [D_i \times \mathbf{1}(t = \tau)] + \psi_i^p + \delta_t^p + \epsilon_{it}^p$$

[32] Specifically, we estimate the following variant of equation (2)

$$E_{it}^p = \beta_1^p [D_i \times t] + \sum_i \beta_{2i}^p [D_i \times \mathbf{1}(t \geq 2013) \times t] + \psi_i^p + \delta_t^p + \epsilon_{it}^p$$

where β_{2i}^p is the post-C&T trend break for zip code i. Figures 4 and S5 plot $\frac{\beta_{2i}^p}{\beta_1^p} * 100$, the percentage change in the EJ gap trend following the introduction of the C&T program for zip code i relative to the average pre-C&T EJ gap trend across disadvantaged zip codes.

Table 2: Trend break in the environmental justice gap

	(1) $PM_{2.5}$	(2) PM_{10}	(3) NO_x	(4) SO_x
β_1^p	0.042	0.065	0.085	0.037
	(0.015)	(0.017)	(0.037)	(0.025)
	[0.006]	[0.000]	[0.026]	[0.151]
β_2^p	-0.063	-0.090	-0.143	-0.101
	(0.022)	(0.029)	(0.074)	(0.051)
	[0.006]	[0.003]	[0.060]	[0.053]
$\beta_1^p + \beta_2^p$	-0.021	-0.026	-0.058	-0.064
	(0.015)	(0.020)	(0.050)	(0.027)
	[0.159]	[0.203]	[0.252]	[0.024]
$(\beta_2^p/\beta_1^p) * 100$	-149.699	-139.739	-168.282	-272.291
	(36.368)	(29.971)	(53.375)	(66.043)
	[0.000]	[0.000]	[0.002]	[0.000]
Zip codes	1649	1649	1649	1649
Counties	58	58	58	58
Observations	16,416	16,416	16,416	16,416

NOTES: Estimates of the pre-C&T EJ gap trend (i.e., β_1^p from equation (2)), the post-C&T EJ gap trend break (i.e., β_2^p from equation (2)), the post-C&T EJ gap trend (i.e, $\beta_1^p + \beta_2^p$), and the percentage change in the EJ gap trend following the introduction of the C&T program (i.e., $\frac{\beta_2^p}{\beta_1^p} * 100$) for $PM_{2.5}$, PM_{10}, NO_x, and SO_x, across columns. All models include zip code-specific and year-specific dummy variables. Observations weighted by zip code-level average population during 2008-2012. Parentheses indicate standard errors that account for statistical uncertainty in C&T predicted emissions (μ_{it}^p from equation (1) via the bootstrap procedure in Appendix A.1) and county-level heterogeneity in EJ gap effects of arbitrary form (ϵ_{it}^p from equation (2)). P-value in brackets.

Robustness checks We subject our EJ gap trend effects to several robustness checks. Most robustness checks forgo the bootstrap procedure across steps 1-3 (detailed in Appendix A.1) given the computational demands of that procedure. Instead, Figure 5 presents only point estimates of the percentage change in the EJ gap trend following C&T (i.e., $\frac{\beta_2^p}{\beta_1^p} * 100$) for each robustness check and compares that with the point estimate and 95% confidence interval of our benchmark result for which inference does account for statistical uncertainty

Figure 3: Environmental justice gap before and after the cap-and-trade program

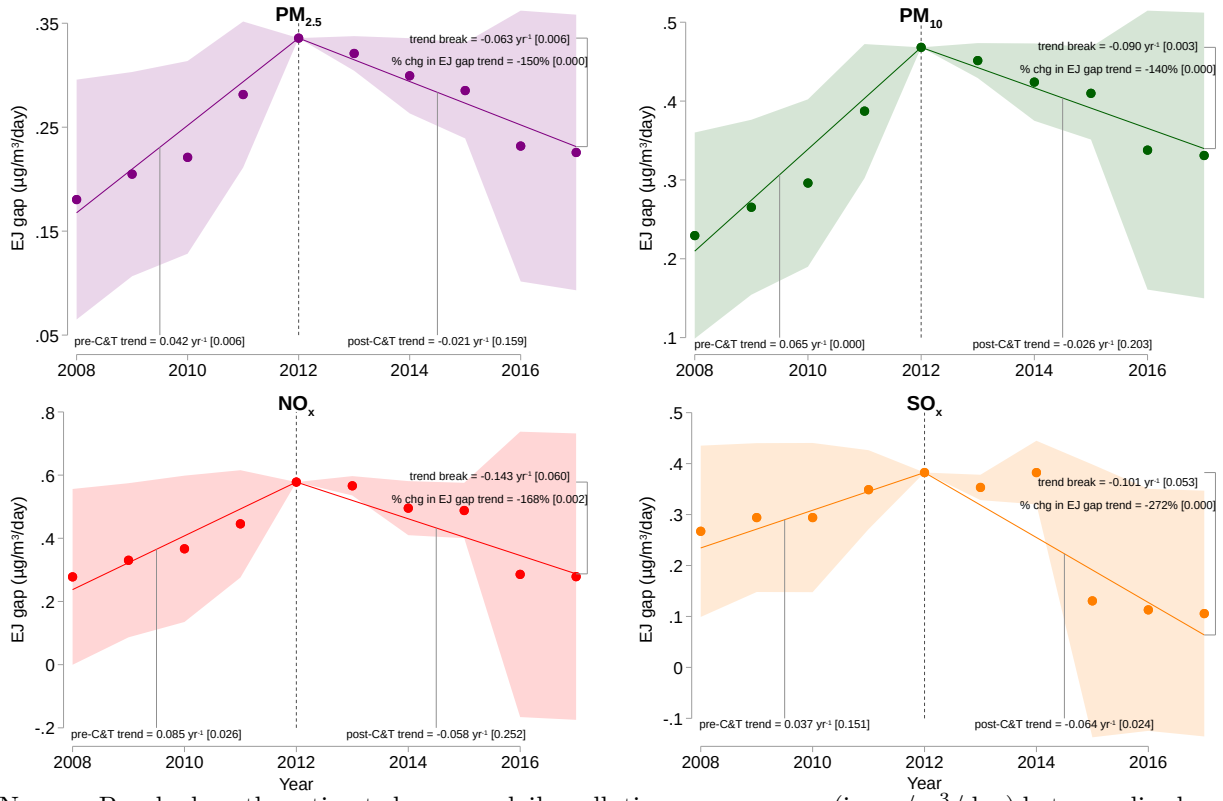

NOTES: Panels show the estimated average daily pollution exposure gap (in $\mu g/m^3$/day) between disadvantaged and other zip codes (i.e., "EJ gap") during 2008-2017 for $PM_{2.5}$, PM_{10}, NO_x, and SO_x, respectively. Dots show year-specific EJ gap. Solid lines show linear fit for EJ gap trend before (2008-2012) and after (2013-2017) the C&T program. Associated text indicates point estimates and standard errors for the pre-C&T linear trend, post-C&T trend break, post-C&T linear trend, and the percentage change in the EJ gap trend (i.e., β_1^p, β_2^p, $\beta_1^p + \beta_2^p$, $\frac{\beta_2^p}{\beta_1^p} * 100$). 95% confidence interval and p-values (in brackets) account for statistical uncertainty in C&T predicted emissions (μ_{it}^p from equation (1) via the bootstrap procedure in Appendix A.1) and county-level heterogeneity in EJ gap effects of arbitrary form (ϵ_{it}^p from equation (2)). Trend break estimates also reported in Table 2.

in equation (1) via our bootstrap procedure.[33]

Within step 1, we conduct six robustness checks. Equation (1) models changes in the emissions difference between C&T regulated and non-regulated facility as linear trends. We find a similar result when we estimate a more flexible version of equation (1) with year-specific emission differences (M2 of Figure 5 and column 1 of Table S7). Next, we consider restricting facilities to those with sample average annual GHG emissions below the 70th and 80th percentiles, respectively (M3-4 of Figure 5 and columns 2-3 of Table S7, using equation (1) estimates in columns 1 and 3 of Table S2). These alternative facility sample restrictions

[33] Coefficients β_1^p and β_2^p in accompanying Tables S7 and S8 cluster standard errors ϵ_{it}^p from equation (2) at the county-level but are not adjusted for statistical uncertainty in equation (1).

Figure 4: Spatial heterogeneity in EJ gap effects

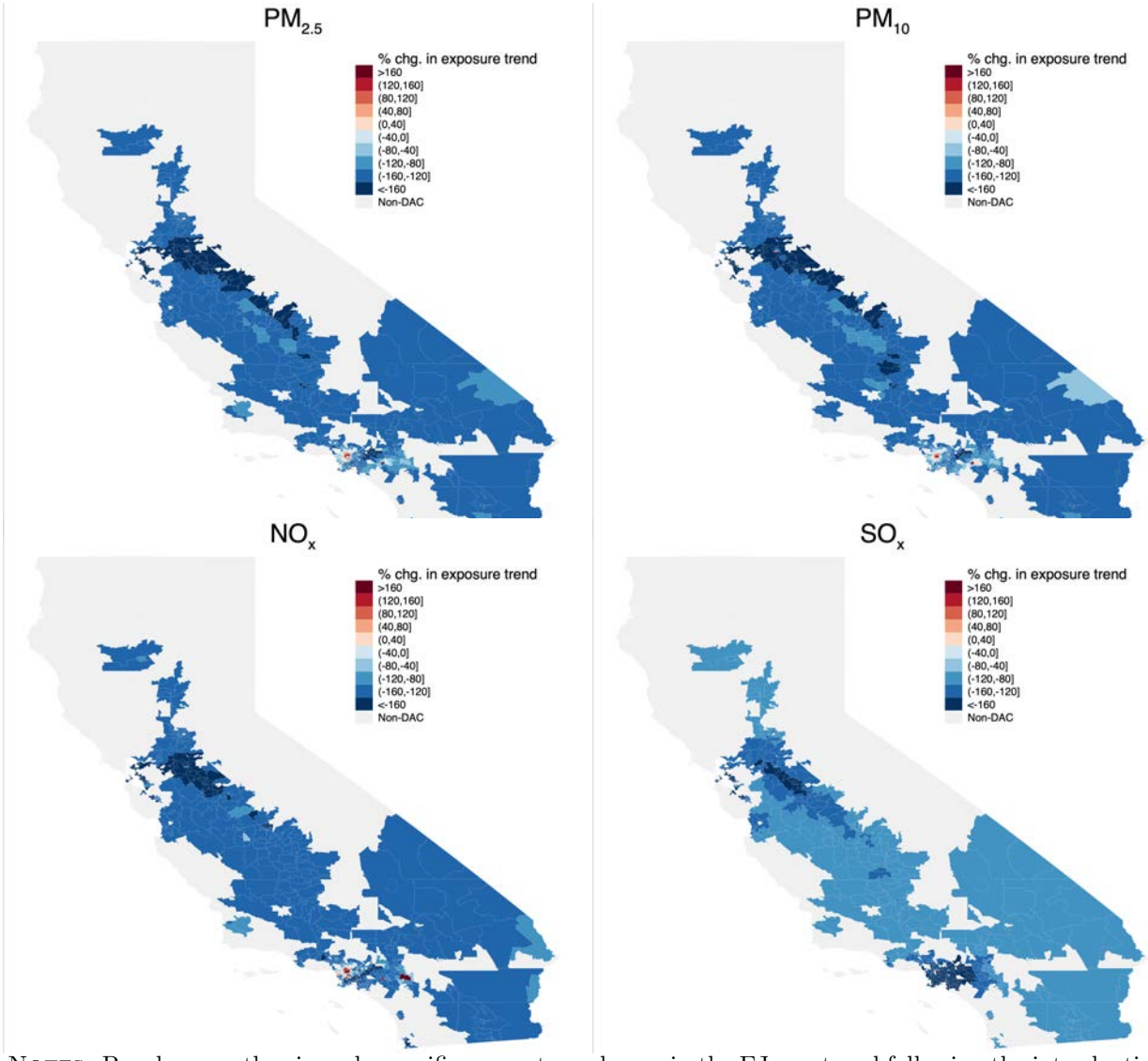

NOTES: Panels maps the zip code-specific percentage change in the EJ gap trend following the introduction of the C&T program for disadvantaged zip codes across $PM_{2.5}$, PM_{10}, NO_x, and SO_x. Blue (red) shading indicates reduced (increased) EJ gap trends following C&T for disadvantaged zip codes. Gray shading shows non-disadvantaged zip codes.

do not alter EJ gap trend effects. We further allow the post C&T emissions trend break to vary as a linear function of sample average emissions, as shown in column 2 of Table S3. For $PM_{2.5}$, PM_{10}, and NO_x, the percentage change in the EJ gap trend has a slightly larger magnitude, consistent with column 2 of Table S3 indicating that our benchmark model, which assumes the same percentage emissions effect across regulated facilities, is understating the level of abatement for facilities that emit more on average. For SO_x, this dimension of heterogeneity implies much larger drops in the post-C&T EJ gap trend. Lastly, we examine

EJ gap effects after restricting the set of unregulated C&T facilities to those in counties under Clear Air Act nonattainment and those whose parent company only operates a single facility (M6-7 of Figure 5 and columns 5 and 6 of Table S7, using equation (1) estimates in columns 2 and 3 of Table S4). SUTVA concerns do not alter EJ gap trend effects.

We conduct four robustness checks within step 2. We use pollution half-life parameters taken from the atmospheric chemistry literature because HYSPLIT does not model pollution decay over time. Our results are relatively stable to whether we allow for a 10% larger half-life parameter which implies a slower decay rate (M8 of Figure 5 and column 1 Table S8) or a 10% smaller half-life parameter which implies a faster decay rate (M9 of Figure 5 and column 2 of Table S8). Likewise our results are little affected when we lower the height of the planetary boundary layer to 0.5 km (M10 of Figure 5 and column 3 Table S8) or raise it to 2 km (M11 of Figure 5 and column 4 Table S8).

We conduct three robustness checks within step 3. The first set of checks consider alternative error structures for ϵ^p_{it}. We find that precision increases when we allow ϵ^p_{it} to be spatially correlated within a uniform kernel across a distance of 500 km distance (Conley, 1999), roughly the longitudinal width of California, and serially correlated across 5 years (Newey and West, 1987) (column 5 of Table S8). Likewise, precision increases when we allow for error terms to be correlated across the four local pollutants using a Seemingly Unrelated Regression (SUR) procedure (column 6 of Table S8). Equation (2) examines the EJ gap in daily pollution levels of μg/m^3/day, the unit of exposure typically used for air pollution policy and by the public health literature. In Table S9, we detect a post-C&T EJ gap trend break after applying an inverse hyperbolic sine transformation to our outcome variable, showing C&T-driven exposure in disadvantaged communities decreased as a percentage of exposure in other communities after 2013. Standard errors reported in Table S9 are adjusted for statistical uncertainty from equation (1) using our bootstrap procedure.

Finally, to examine the potential role of secondary $PM_{2.5}$, we replace HYSPLIT in step 2 of our procedure with InMAP, a reduced-complexity dispersal model based on output from WRF-Chem, which incorporates atmospheric chemistry in order to model total (i.e., primary and secondary) $PM_{2.5}$ exposure from C&T-driven facility-level $PM_{2.5}$, NO_x, and SO_x, emissions (Tessum, Hill and Marshall, 2017).[34] InMAP, however, has one major limitation: it uses dispersal patterns in 2005, whereas our sample period is 2008-2017. Because InMAP does not model dispersal patterns during our sample period, we are unable to directly compare

[34] In addition to the inputs used in HYSPLIT, InMap requires the diameter, temperature, and emissions velocity for each smokestack. We obtained these inputs from CARB. In the case of facilities with more than one stack, we use the mean value across stacks. In the case of facilities with missing observations, we use the industry-level average.

Figure 5: Robustness checks for EJ gap effects

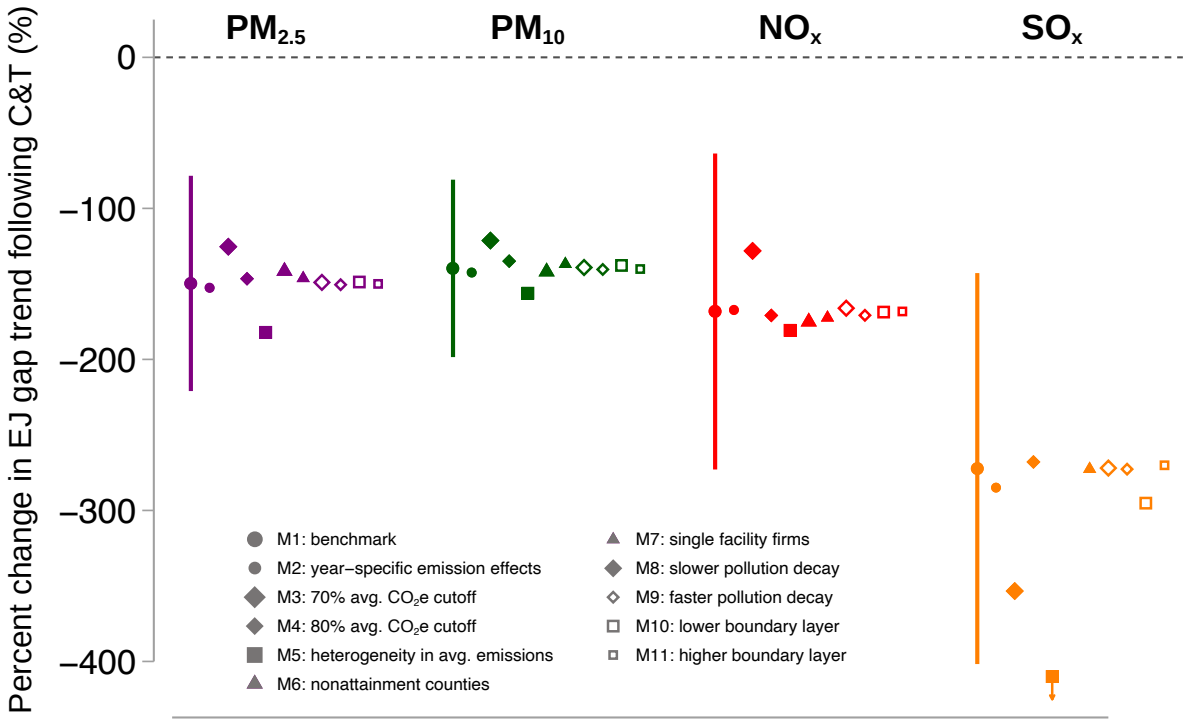

NOTES: Percentage change in the EJ gap trend following the introduction of the C&T program (i.e., $\frac{\beta_2^p}{\beta_1^p} * 100$) for $PM_{2.5}$, PM_{10}, NO_x, and SO_x across robustness checks. M1: benchmark model point estimate and 95% confidence interval accounting for uncertainty in equations (1) and (2). Point estimate shown for all other models. M2: using year-specific effects to estimate C&T-driven emissions. M3: restricting sample to facilities with average annual GHG emissions below the 70th percentile. M4: restricting sample to facilities with average annual GHG emissions below the 80th percentile. M5: allowing heterogeneous emissions effects by average annual emissions. M6: restricting unregulated facilities to those in counties under Clear Air Act nonattainment. M7: restricting unregulated facilities to those whose parent company only operates a single plant. M8: applying a slower pollution decay (i.e., 10% larger half-life parameter). M9: applying a faster pollution decay (i.e., 10% smaller half-life parameter). M10: applying a planetary boundary layer set at 0.5 km. M11: applying planetary boundary layer set at 2 km. Point estimates also reported in Tables S7-S8.

estimates using InMAP-generated exposure with that using HYSPLIT-generated exposure.[35] Instead, we examine the role of secondary $PM_{2.5}$ by comparing how EJ gap trend estimates differ between InMAP-generated primary $PM_{2.5}$ exposure and InMAP-generated total $PM_{2.5}$ exposure. If these two sets of estimates using InMap are similar, it is plausible that the true EJ gap effects for secondary $PM_{2.5}$ are similar to effects using HYSPLIT-generated primary $PM_{2.5}$ exposure. Table S10 replicates the structure of Table 2. Column 1 examines InMAP-

[35] Furthermore, there is a difference in units between HYSPLIT and InMap. For any given location, HYSPLIT produces the stock of pollution exposure during a given period, whereas InMAP produces that period's average flow of pollution exposure.

generated primary $PM_{2.5}$ exposure while column 2 examines InMAP-generated total $PM_{2.5}$ exposure. EJ gap trend effects are very similar across these two columns.

The importance of modeling pollution dispersal Our empirical approach explicitly embeds an atmospheric dispersal model within a causal inference framework. Compared with conventional methods for assigning pollution exposure from emission sources, this approach lends two benefits. It accounts for actual pollution dispersal patterns as dictated by topography and time-varying meteorological conditions. It also determines resulting pollution exposure across all locations in California, rather than a subset of locations assumed to be exposed to policy-driven emissions. To explicitly demonstrate the importance of accounting for pollution dispersal for our results, we now compare estimates from using our approach with that of more conventional methods of assigning pollution exposure from emission sources.

Figure 6: Importance of modeling pollution dispersal

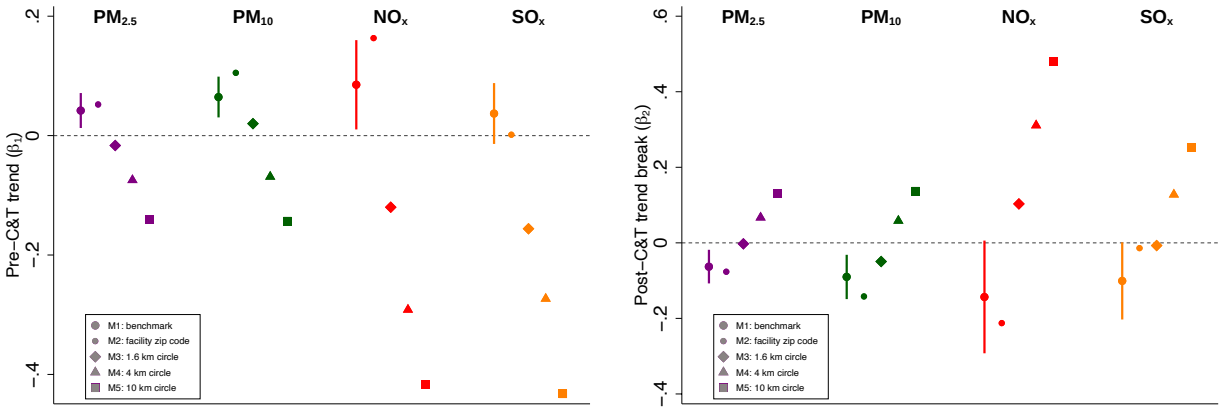

NOTES: Left panel shows estimates of pre-C&T trend (i.e., β_1^p) and right panel shows estimates of post-C&T trend break (i.e., β_2^p) for $PM_{2.5}$, PM_{10}, NO_x, and SO_x across different methods for assigning pollution exposure from emissions. M1: benchmark model with point estimate and 95% confidence interval accounting for uncertainty in equations (1) and (2). Point estimate shown for all other models. M2: pollution exposure assigned only to zip code of emitting facility. M3-5: pollution exposure assigned to zip codes with centroid within 1.6 km, 4 km and 10 km circle of emitting facility, respectively. Point estimates also reported in Table S11.

Figure 6 plots estimates of the pre-C&T trend, or β_p^1 (left panel), and the post-C&T trend break, or β_p^2 (right panel), across criteria pollutants under different assumptions about how facility-level emissions alter location-specific exposure.[36] In M1, we show our benchmark estimate where pollution dispersal is modeled by HYSPLIT every 4 hours throughout the

[36]Unlike Figure 5, Figure 6 does not plot $\frac{\beta_2^p}{\beta_1^p} * 100$ because β_1^p and β_2^p do not have consistent sign across the different methods for assigning emissions to exposure.

2008-2017 period. In M2 (and column 1 of Table S11), we assume that pollution exposure from a facility is limited to the zip code of that facility, referred to in the literature as "unit-hazard coincidence" (Banzhaf, Ma and Timmins, 2019). In M3-5 (and columns 2-4 of Table S11), we employ a distance-based measure by assuming that pollution exposure from a facility is limited to zip codes with centroids that are within 1.6, 4, and 10 km circles around the facility. These radial distances appear in the literature but nonetheless are chosen largely arbitrarily. Point estimates of β_p^1 and β_p^2 vary greatly across these alternative methods for assigning pollution exposure. Not only do some estimates fall well outside the 95% confidence intervals of our benchmark results, they also have different signs.

6 Discussion

Many market settings are characterized by efficiency-equity tradeoffs. We find that California's carbon market led to an equity co-benefit by narrowing the pollution exposure gap between disadvantaged and other communities. This result brings causal evidence to a long-standing debate that continues to shape one of the world's most ambitious climate policies. Moreover, the integration of pollution dispersal modeling and causal inference developed in this paper to map program-driven emissions onto pollution exposure may have broader applications across a variety of environmental valuation questions.

Equity concerns regarding California's cap-and-trade program remain. First, while we show that the program has led the pollution exposure gap between disadvantaged and other communities to fall, this gap has not been eliminated five years into the program. Second, pollution exposure constitutes only one component of the many distributional consequences of California's cap-and-trade program. Questions remain regarding how the program may have altered the distribution of health outcomes as well as the distribution of the program's cost burden. A comprehensive understanding of welfare inequality must also account for sorting as households move in response to changes in the pollution exposure gap (Depro, Timmins and O'Neil, 2015; Banzhaf, Ma and Timmins, 2019). Third, a broader notion of equity must also consider the ability of disadvantaged communities to partake in decision-making around environmental policies. Such procedural justice issues remain in California though recent policies such as AB 617 are beginning to engage disadvantaged communities directly in local pollution regulation design (Fowlie, Walker and Wooley, 2020).

More generally, despite these findings for California, market-based environmental policies should not be used explicitly to address environmental justice concerns. Market-based policies are intended for allocative efficiency and not distributional objectives, per se. The EJ gap consequences detected in California emerges from the state's spatial distribution of

polluting facilities and demographic characteristics. In other settings where facilities with steeper marginal abatement cost curves are upwind of disadvantaged communities, an environmental market could increase the environmental justice gap. Given the difficulties with observing facility-level marginal abatement cost curves, it is hard to anticipate ex-ante how market-based policies will alter existing EJ gaps. As a safeguard, market-based policies should therefore be considered in tandem with policies that specifically address environmental justice concerns. In short, environmental justice problems need environmental justice policies.

References

Ash, Michael, and T. Robert Fetter. 2004. "Who Lives on the Wrong Side of the Environmental Tracks? Evidence from the EPA's Risk-Screening Environmental Indicators Model." *Social Science Quarterly*, 85(2): 441–462.

Banzhaf, Spencer, Lala Ma, and Christopher Timmins. 2019. "Environmental Justice: The Economics of Race, Place, and Pollution." *Journal of Economic Perspectives*, 33(1): 185–208.

Baumol, William J., and Wallace E. Oates. 1988. *The Theory of Environmental Policy, Second Edition.* Cambridge University Press.

Bellemare, Marc F, and Casey J Wichman. 2020. "Elasticities and the inverse hyperbolic sine transformation." *Oxford Bulletin of Economics and Statistics*, 82(1): 50–61.

Borenstein, Severin, James Bushnell, Frank A. Wolak, and Matthew Zaragoza-Watkins. 2019. "Expecting the Unexpected: Emissions Uncertainty and Environmental Market Design." *American Economic Review*, 109(11): 3953–77.

Bowen, William. 2002. "An Analytical Review of Environmental Justice Research: What do we Really Know?" *Environmental Management*, 29(1): 3–15.

Bullard, Robert. 2000. *Dumping in Dixie: Race, Class, and Environmental Quality.* Westview Press.

Burtraw, Dallas, A Carlson, D Cullenward, Q Foster, and M Fowlie. 2018. "2018 Annual Report of the Independent Emissions Market Advisory Committee."

Burtraw, Dallas, David A Evans, Alan Krupnick, Karen Palmer, and Russell Toth. 2005. "Economics of Pollution Trading for SO2 and NO x." *Annu. Rev. Environ. Resour.*, 30: 253–289.

Casey, Joan A, Jason G Su, Lucas RF Henneman, Corwin Zigler, Andreas M Neophytou, Ralph Catalano, Rahul Gondalia, Yu-Ting Chen, Leanne Kaye, Sarah S Moyer, et al. 2020. "Improved asthma outcomes observed in the vicinity of coal power plant retirement, retrofit and conversion to natural gas." *Nature Energy*, 5(5): 398–408.

Colmer, Jonathan, Ralf Martin, Mirabelle Muûls, Ulrich J Wagner, et al. 2020. "Does pricing carbon mitigate climate change? Firm-level evidence from the European Union emissions trading scheme." *Center for Economic Performance Discussion Paper*, , (1728).

Conley, Timothy G. 1999. "GMM Estimation with Cross Sectional Dependence." *Journal of Econometrics*, 92(1): 1–45.

Costello, Christopher, Daniel Ovando, Tyler Clavelle, C. Kent Strauss, Ray Hilborn, Michael C. Melnychuk, Trevor A. Branch, Steven D. Gaines, Cody S. Szuwalski, Reniel B. Cabral, Douglas N. Rader, and Amanda Leland. 2016. "Global Fishery Prospects under Contrasting Management Regimes." *Proceedings of the National Academy of Sciences*, 113(18): 5125–5129.

Crocker, T. 1966. "The structuring of atmospheric pollution control systems. The economics of air pollution." *The economics of air pollution. New York, WW Norton & Co*, 61–86.

Cummiskey, Kevin, Chanmin Kim, Christine Choirat, Lucas R. F. Henneman, Joel Schwartz, and Corwin Zigler. 2019. "A Source-Oriented Approach to Coal Power Plant Emissions Health Effects."

Currie, Janet, John Voorheis, and Reed Walker. 2020. "What Caused Racial Disparities in Particulate Exposure to Fall? New Evidence from the Clean Air Act and Satellite-Based Measures of Air Quality." National Bureau of Economic Research Working Paper 26659.

Cushing, Lara, Dan Blaustein-Rejto, Madeline Wander, Manuel Pastor, James Sadd, Allen Zhu, and Rachel Morello-Frosch. 2018. "Carbon Trading, Co-pollutants, and Environmental Equity: Evidence from California's cap-and-trade program (2011–2015)." *PLoS medicine*, 15(7): e1002604.

Dale, John H. 1968. "Pollution, Property, and Prices: An Essay in Policy-Making."

Dales, John H. 1968. *Pollution, Property and Prices: An Essay in Policy.* Toronto: University of Toronto Press.

Davis, Lucas, and Catherine Hausman. 2016. "Market Impacts of a Nuclear Power Plant Closure." *American Economic Journal: Applied Economics*, 8(2): 92–122.

Depro, Brooks, Christopher Timmins, and Maggie O'Neil. 2015. "White Flight and Coming to the Nuisance: Can Residential Mobility Explain Environmental Injustice?" *Journal of the Association of Environmental and Resource Economists*, 2(3): 439–468.

Deschenes, Olivier, and Kyle C Meng. 2018. "Quasi-experimental Methods in Environmental Economics: Challenges and Opportunities." *Handbook of Environmental Economics*, 4: 285.

Draxler, Roland R, and GD Hess. 1998. "An Overview of the HYSPLIT$_4$ Modelling System for Trajectories." *Australian Meteorological Magazine*, 47(4): 295–308.

EPA, US. 2015. "Revision to the Guideline on Air Quality Models: Enhancements to the AERMOD Dispersion Modeling System and Incorporation of Approaches to Address Ozone and Fine Particulate Matter." US Environmental Protection Agency Working Paper 2060-AS54.

Fowlie, Meredith, Reed Walker, and David Wooley. 2020. "Climate policy, environmental justice, and local air pollution." Brookings Economic Studies.

Fowlie, Meredith, Stephen P. Holland, and Erin T. Mansur. 2012. "What Do Emissions Markets Deliver and to Whom? Evidence from Southern California's NO_x Trading Program." *American Economic Review*, 102(2): 965–93.

Graff Zivin, Joshua, and Matthew Neidell. 2013. "Environment, health, and human capital." *Journal of Economic Literature*, 51(3): 689–730.

Grainger, Corbett, and Thanicha Ruangmas. 2018. "Who Wins from Emissions Trading? Evidence from California." *Environmental and Resource Economics*, 71(3): 703–727.

Greenstone, Michael, and Ted Gayer. 2009. "Quasi-experimental and Experimental Approaches to Environmental Economics." *Journal of Environmental Economics and Management*, 57(1): 21 – 44. Frontiers of Environmental and Resource Economics.

Henneman, Lucas RF, Loretta J Mickley, and Corwin M Zigler. 2019. "Air pollution accountability of energy transitions: the relative importance of point source emissions and wind fields in exposure changes." *Environmental Research Letters*, 14(11): 115003.

Herron, Elise. 2019. "Oregon Clean Energy Jobs Bill Has Mixed Support From Environmental Justice Groups." *Willamette Week*.

Kim, Chanmin, Lucas RF Henneman, Christine Choirat, and Corwin M Zigler. 2020. "Health effects of power plant emissions through ambient air quality." *Journal of the Royal Statistical Society: Series A (Statistics in Society)*.

Leber, Rebecca. 2016. "The most Dramatic Climate Fight of the Election is in Washington State." *Grist*.

Lee, Chulkyu, Randall V Martin, Aaron van Donkelaar, Hanlim Lee, Russell R Dickerson, Jennifer C Hains, Nickolay Krotkov, Andreas Richter, Konstantine Vinnikov, and James J Schwab. 2011. "SO_2 Emissions and Lifetimes: Estimates from Inverse Modeling using in situ and global, space-based (SCIAMACHY and OMI) Observations." *Journal of Geophysical Research: Atmospheres*, 116(D6).

Liu, Fei, Steffen Beirle, Qiang Zhang, Steffen Dörner, Kebin He, and Thomas Wagner. 2016. "NO_x Lifetimes and Emissions of Cities and Power Plants in Polluted Background Estimated by Satellite Observations." *Atmospheric Chemistry and Physics*, 16(8): 5283–5298.

Mansur, Erin T., and Glenn Sheriff. 2019. "Do Pollution Markets Harm Low Income and Minority Communities? Ranking Emissions Distributions Generated by California's RECLAIM Program." National Bureau of Economic Research Working Paper 25666.

Martin, Ralf, Mirabelle Muûls, and Ulrich J Wagner. 2016. "The impact of the European Union Emissions Trading Scheme on regulated firms: what is the evidence after ten years?" *Review of environmental economics and policy*, 10(1): 129–148.

Mohai, Paul, David Pellow, and J. Timmons Roberts. 2009. "Environmental Justice." *Annual Review of Environment and Resources*, 34(1): 405–430.

Montgomery, W. David. 1972. "Markets in Licenses and Efficient Pollution Control Programs." *Journal of Economic Theory*, 5(3): 395 – 418.

Morello-Frosch, Rachel, and Bill M Jesdale. 2006. "Separate and Unequal: Residential Segregation and Estimated Cancer Risks Associated with Ambient Air Toxics in US Metropolitan Areas." *Environmental Health Perspectives*, 114(3): 386.

Newey, Whitney K., and Kenneth D. West. 1987. "A Simple, Positive Semi-Definite, Heteroskedasticity and Autocorrelation Consistent Covariance Matrix." *Econometrica*, 55(3): 703–708.

Petrick, Sebastian, and Ulrich J Wagner. 2014. "The impact of carbon trading on industry: Evidence from German manufacturing firms." *Available at SSRN 2389800*.

Rahn, David A., and Christopher J. Mitchell. 2016. "Diurnal Climatology of the Boundary Layer in Southern California Using AMDAR Temperature and Wind Profiles." *Journal of Applied Meteorology and Climatology*, 55(5): 1123–1137.

Ringquist, Evan J. 2005. "Assessing Evidence of Environmental Inequities: A Meta-analysis." *Journal of Policy Analysis and Management*, 24(2): 223–247.

Salzman, James, Genevieve Bennett, Nathaniel Carroll, Allie Goldstein, and Michael Jenkins. 2018. "The Global Status and Trends of Payments for Ecosystem Services." *Nature Sustainability*, 1(3): 136–144.

Schmalensee, Richard, and Robert N. Stavins. 2019. "Policy Evolution under the Clean Air Act." *Journal of Economic Perspectives*, 33(4): 27–50.

Shapiro, Joseph S, and Reed Walker. 2021. "Where is Pollution Moving? Environmental Markets and Environmental Justice." National Bureau of Economic Research Working Paper 28389.

Sullivan, Daniel M. 2017. "The True Cost of Air Pollution: Evidence from the Housing Market." *mimeo*.

Tessum, Christopher W., Jason D. Hill, and Julian D. Marshall. 2017. "InMAP: A model for air pollution interventions." *PLOS ONE*, 12(4): 1–26.

Tessum, Christopher W., Joshua S. Apte, Andrew L. Goodkind, Nicholas Z. Muller, Kimberley A. Mullins, David A. Paolella, Stephen Polasky, Nathaniel P. Springer, Sumil K. Thakrar, Julian D. Marshall, and Jason D. Hill. 2019. "Inequity in consumption of goods and services adds to racial–ethnic disparities in air pollution exposure." *Proceedings of the National Academy of Sciences*, 116(13): 6001–6006.

Transnational Institute. 2013. "It is Time to Scrap the ETS! ."

U.S. EPA. 2018. "User's Guide for the AMS/EPA Regulatory Model AERMOD."

World Bank Group. 2019. "State and Trends of Carbon Pricing."

A Appendix Methods

A.1 Bootstrap procedure for incorporating uncertainty in C&T emission effects

This section details our bootstrap procedure over steps 1-3 to account for statistical uncertainty in C&T-driven emission effects from equation (1), reproduced here:

$$asinh(Y_{jt}^p) = \kappa_1^p[C_j \times t] + \kappa_2^p[C_j \times \mathbf{1}(t \geq 2013) \times t] + \phi_j^p + \gamma_t^p + \mu_{jt}^p$$

We obtain point estimates $\widehat{\kappa}_1^p$, $\widehat{\kappa}_2^p$ and standard errors $\widehat{\sigma}_{\kappa_1^p}$ and $\widehat{\sigma}_{\kappa_2^p}$ from equation (1). We then iterate the following procedure for draws $b = 1...250$:

1. Draw $\widehat{\kappa}_1^p(b) \sim N(\widehat{\kappa}_1^p, \widehat{\sigma}_{\kappa_1^p})$ and $\widehat{\kappa}_2^p(b) \sim N(\widehat{\kappa}_2^p, \widehat{\sigma}_{\kappa_2^p})$
2. Construct $\widehat{Y}_{jt}^p(b) = sinh\left(\widehat{\kappa}_1^p(b)[C_j \times t] + \widehat{\kappa}_2^p(b)[C_j \times \mathbf{1}(t \geq 2013) \times t] + \widehat{\phi}_j^p\right) * e^{(RMSE)^2/2)}$, where RMSE is the root mean squared error from equation (1)
3. Feed $\widehat{Y}_{jt}^p(b)$ into HYSPLIT to generate zip code-by-year pollution exposure, $E_{it}^p(b)$
4. Estimate equation (2) using $E_{it}^p(b)$ as the outcome variable to obtain $\widehat{\beta}_1^p(b)$ and $\widehat{\beta}_2^p(b)$

Figure S4 plots the empirical distributions for $\widehat{\beta}_1^p(b)$ and $\widehat{\beta}_2^p(b)$ for $p \in \{PM_{2.5}, PM_{10}, NO_x, SO_x\}$. Denote standard errors across 250 bootstrap runs as $\widehat{\sigma}_{\beta_1^p}(\mu_{jt}^p)$ and $\widehat{\sigma}_{\beta_2^p}(\mu_{jt}^p)$ where the μ_{jt}^p argument indicates the dependence on statistical uncertainty from equation (1). Denote $\widehat{\sigma}_{\beta_1^p}(\epsilon_{jt}^p)$ as the estimated standard error arising from heterogeneity in β_1^p obtained by directly estimating equation (2) with county-level clustered errors. Our reported standard error for β_1^p is $\widehat{\sigma}_{\beta_1^p} = \widehat{\sigma}_{\beta_1^p}(\epsilon_{jt}^p) + \widehat{\sigma}_{\beta_1^p}(\mu_{jt}^p)$. Likewise, for β_2^p. $\widehat{\sigma}_{\beta_1^p}$ and $\widehat{\sigma}_{\beta_2^p}$ are reported in Table 2 and used to construct the confidence intervals displayed in Figure 3.

Appendix Figures

Figure S1: Emissions robustness: placebo C&T program timing

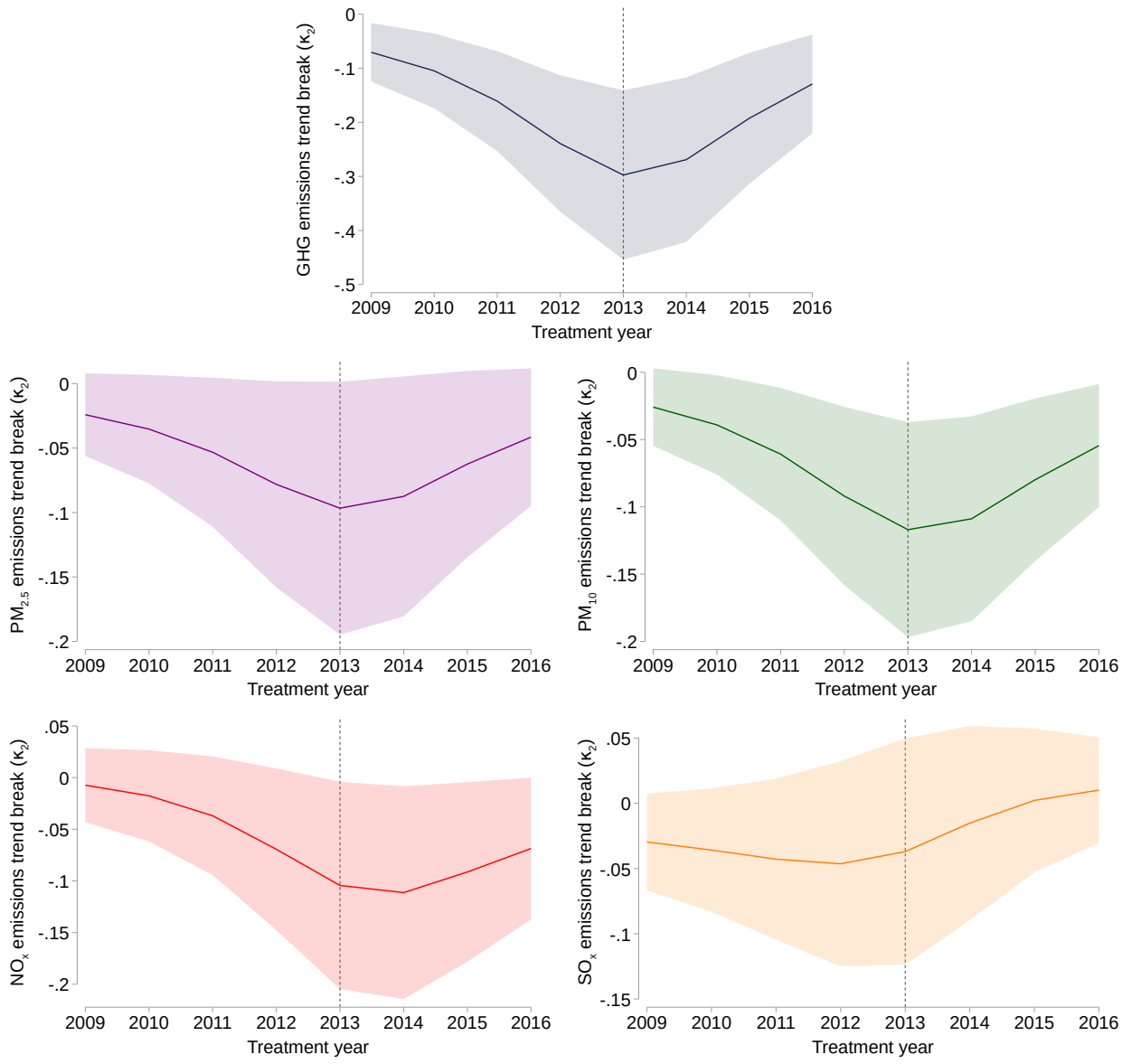

NOTES: Panels show estimated (true and placebo) emissions trend break coefficients (i.e., κ_2 from eq. (1)) for GHG, $PM_{2.5}$, PM_{10}, NO_x, and SO_x emissions from varying the start year of the C&T program. Vertical line at 2013 indicates actual introduction of the program. Shaded areas indicate 95% confidence intervals.

Figure S2: Facility-level C&T-driven abatement between 2012-2017

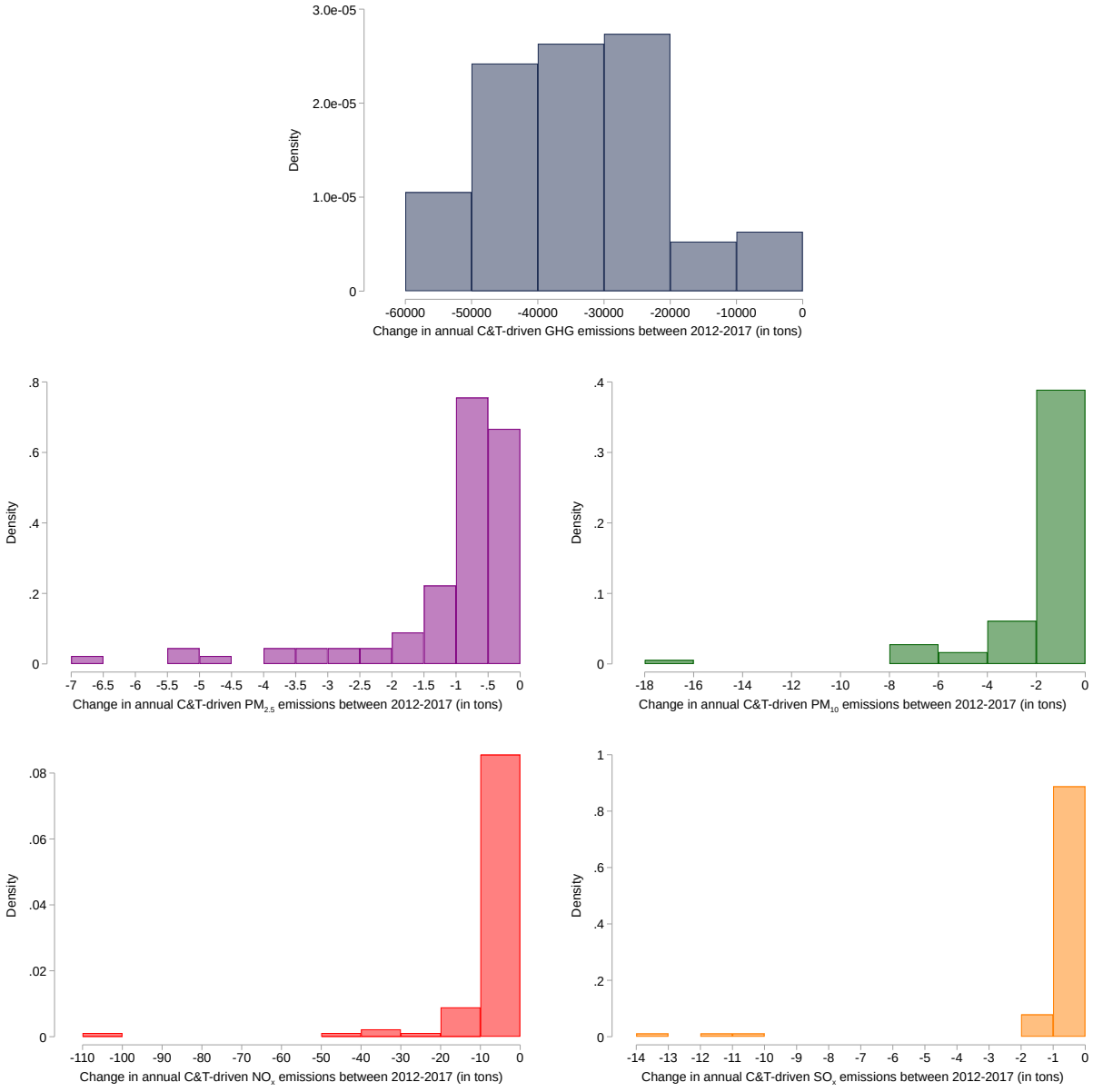

NOTES: Panels show the distribution of facility-level change in C&T-driven pollution between 2012-2017 (or abatement) predicted from step 1 for GHG, $PM_{2.5}$, PM_{10}, NO_x, and SO_x emissions, respectively.

Figure S3: Average pollution exposure driven by C&T regulated facilities

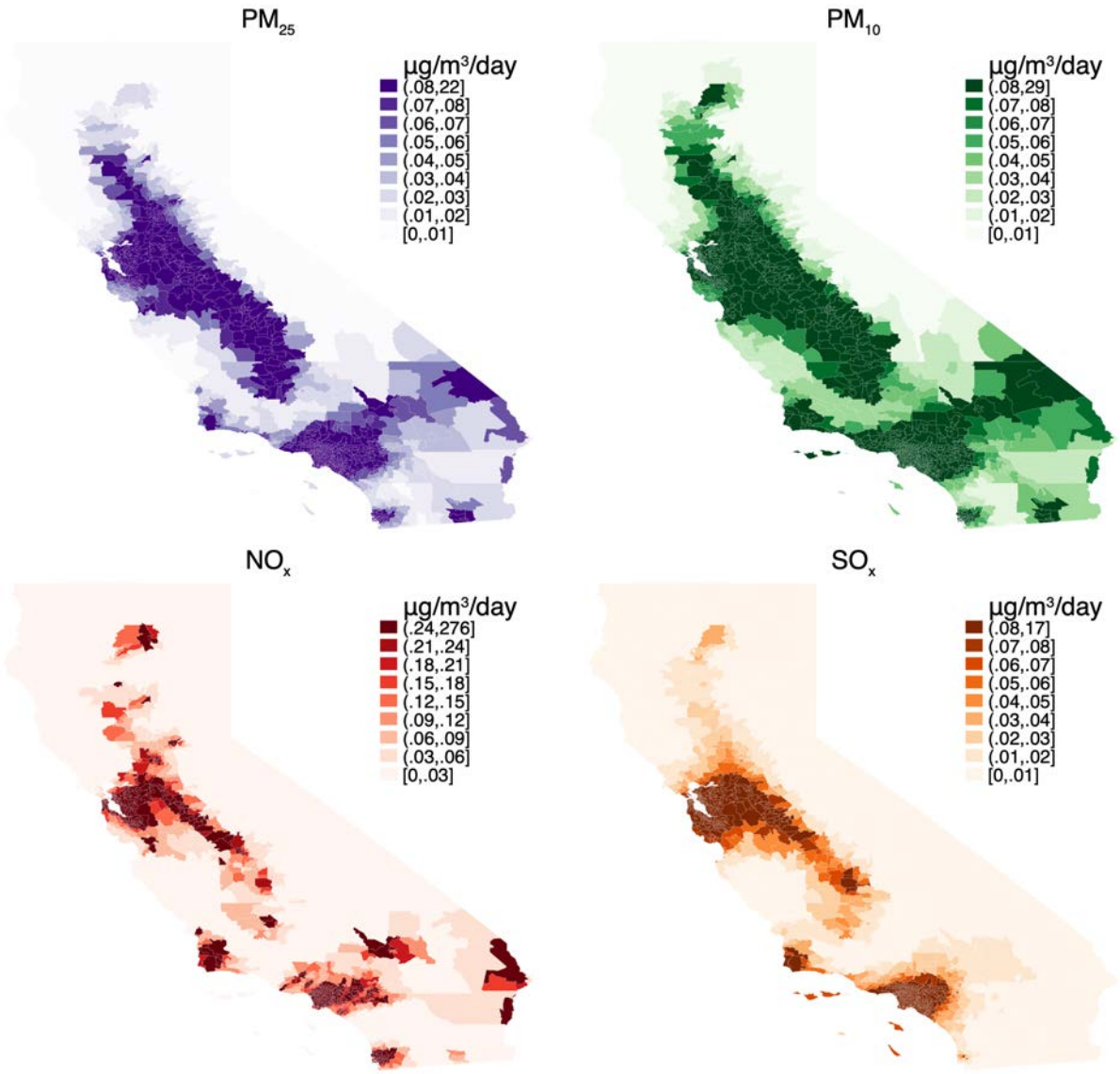

NOTES: Panels show daily exposure (in μg/m^3/day) for each zip code averaged across 2008-2017 from GHG C&T-regulated facilities as modeled in step 2 by HYSPLIT for $PM_{2.5}$, PM_{10}, NO_x, and SO_x, respectively.

Figure S4: Empirical distribution of β_1^p and β_2^p from bootstrapping step 1

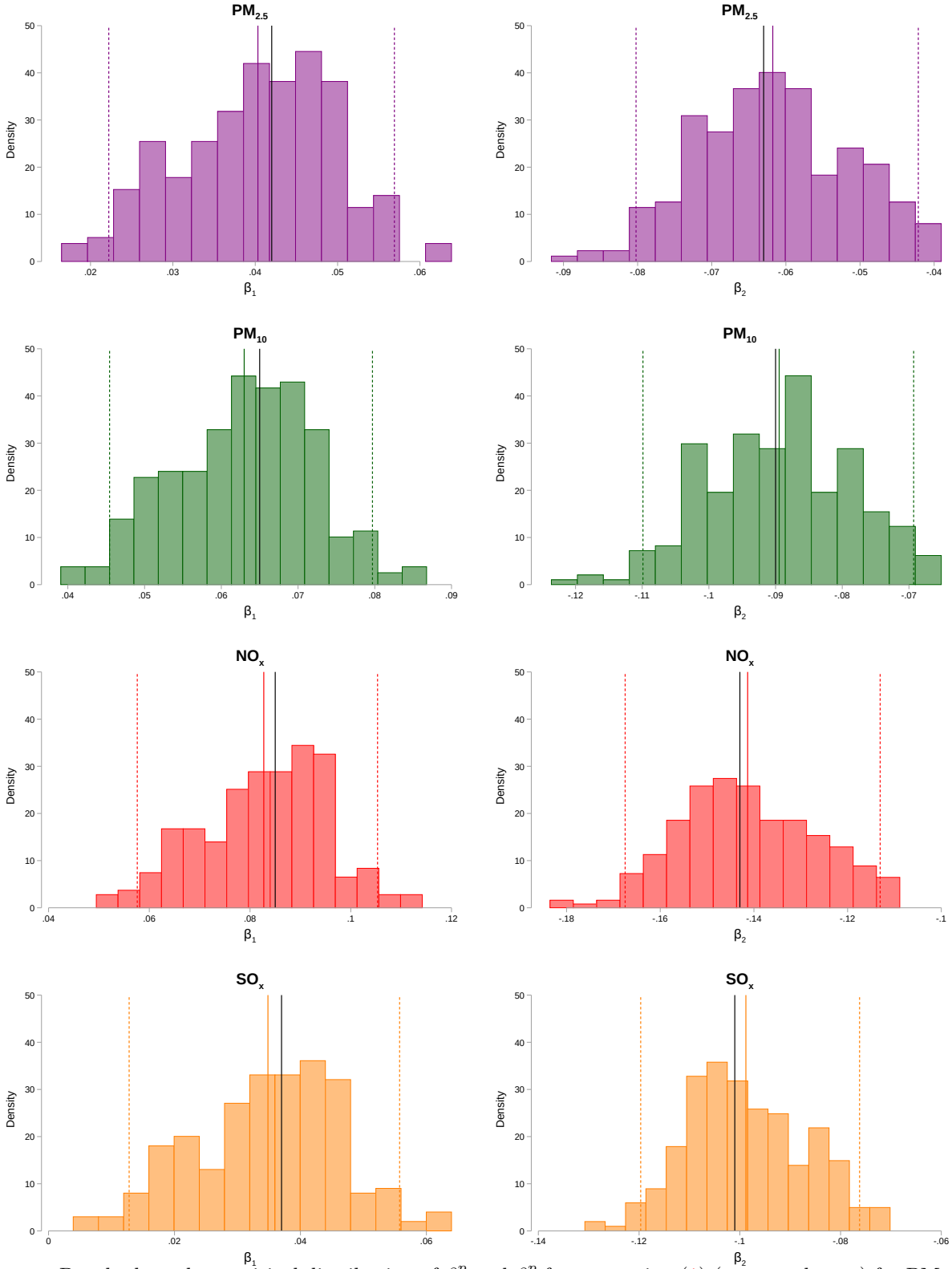

NOTES: Panels show the empirical distribution of β_1^p and β_2^p from equation (1) (across columns) for $PM_{2.5}$, PM_{10}, NO_x, and SO_x (across rows) using the bootstrap procedure detailed in Section A.1 with 250 draws. Solid black line shows parameter from directly estimating equation (1). Solid colored line shows the mean parameter value from the empirical bootstrapped distribution. Dotted colored lines show the 2.5% and 97.5% percentiles of the empirical bootstrap distributions.

Figure S5: Zip code-level percent change in EJ gap trend following C&T

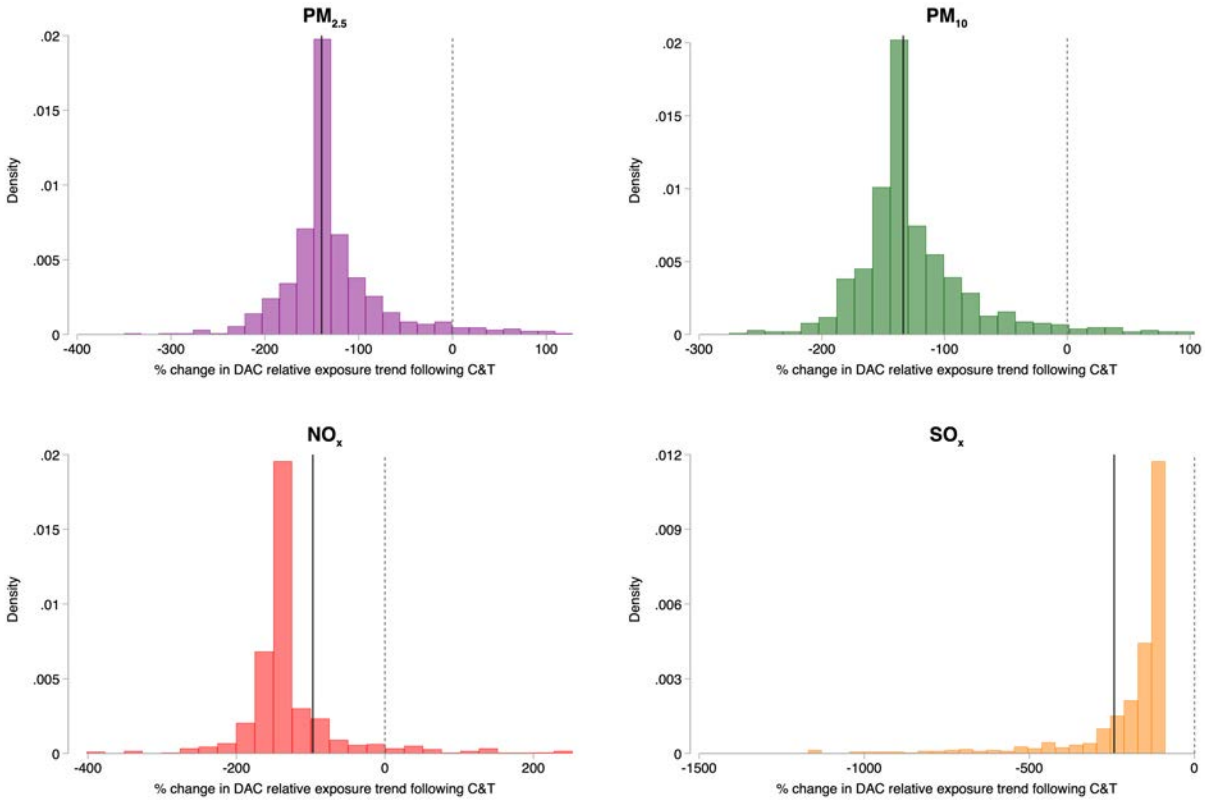

NOTES: Panels show the distribution of zip code-level percentage change in the EJ gap trend following the introduction of the C&T program, for each disadvantaged zip code across $PM_{2.5}$, PM_{10}, NO_x, and SO_x. Solid line shows the average percentage change across disadvantaged zip codes, or $\frac{\beta_2^p}{\beta_1^p} * 100$ from equation (2). Dashed line marks zero.

Appendix Tables

Table S1: GHG cap-and-trade regulated and non-regulated facilities

	C&T regulated facilities	non-C&T regulated facilities
Number	106	227
Shares by sector:		
Agriculture	0	.018
Manufacturing	.629	.498
Mining, oil, and gas extraction	.152	.097
Services	.067	.233
Transportation	.076	.053
Utilities	.076	.093
Wholesale	.01	.009

NOTES: Total number of sample GHG cap-and-trade regulated and non-regulated facilities and by sector shares. Sectors shown adhere to the following definitions: Agriculture: NAICS 11; Manufacturing: NAICS 31-33; Mining, oil, and gas extraction: NAICS 21; Services: NAICS 51, 54, 56, 61, 62, 71, 81, 92; Transportation: NAICS 48, 49; Utilities: NAICS 22; Wholesale: NAICS 42.

Table S2: Emissions robustness: average GHG cutoff

	(1)	(2)	(3)
Avg GHG cutoff (%)	70	75	80
	Outcome is asinh(GHG) emissions		
κ_1^p	0.194	0.187	0.174
	(0.055)	(0.052)	(0.050)
	[0.001]	[0.001]	[0.001]
κ_2^p	-0.307	-0.297	-0.260
	(0.085)	(0.077)	(0.072)
	[0.001]	[0.000]	[0.001]
Facilities	294	316	337
Observations	1,863	2,054	2,234
	Outcome is asinh($PM_{2.5}$) emissions		
κ_1^p	0.071	0.058	0.046
	(0.043)	(0.043)	(0.043)
	[0.111]	[0.183]	[0.298]
κ_2^p	-0.105	-0.097	-0.079
	(0.050)	(0.048)	(0.050)
	[0.044]	[0.053]	[0.121]
Facilities	281	302	323
Observations	1,780	1,968	2,147
	Outcome is asinh(PM_{10}) emissions		
κ_1^p	0.097	0.083	0.075
	(0.034)	(0.033)	(0.035)
	[0.008]	[0.016]	[0.039]
κ_2^p	-0.129	-0.117	-0.103
	(0.043)	(0.039)	(0.041)
	[0.005]	[0.005]	[0.018]
Facilities	281	302	323
Observations	1,780	1,968	2,147
	Outcome is asinh(NO_x) emissions		
κ_1^p	0.085	0.075	0.058
	(0.033)	(0.039)	(0.037)
	[0.015]	[0.061]	[0.128]
κ_2^p	-0.126	-0.104	-0.091
	(0.047)	(0.050)	(0.048)
	[0.010]	[0.042]	[0.066]
Facilities	282	303	324
Observations	1,782	1,970	2,149
	Outcome is asinh(SO_x) emissions		
κ_1^p	-0.005	0.006	-0.004
	(0.038)	(0.035)	(0.035)
	[0.890]	[0.875]	[0.912]
κ_2^p	-0.025	-0.037	-0.020
	(0.048)	(0.043)	(0.045)
	[0.600]	[0.393]	[0.657]
Facilities	282	303	324
Observations	1,777	1,965	2,142

NOTES: Estimates of pre-C&T differential emissions trend (i.e., κ_1^p from equation (1)) and and post-C&T differential emissions trend break (i.e., κ_2^p from equation (1)) for GHG, $PM_{2.5}$, PM_{10}, NO_x, and SO_x across panels. Columns 1, 2, and 3 restrict facilities to those with sample average annual GHG emissions below the 70th, 75th, and 80th percentile, respectively. All models include facility-specific and year-specific dummy variables. Standard errors clustered at the county-level in parentheses, p-value in brackets.

Table S3: Emissions effect robustness: heterogeneity by average emissions

	(1)	(2)	(3)
	Outcome is asinh(GHG) emissions		
κ_1^p	0.187	0.176	0.172
	(0.052)	(0.052)	(0.052)
	[0.001]	[0.002]	[0.002]
κ_2^p	-0.297	-0.361	-0.354
	(0.077)	(0.092)	(0.097)
	[0.000]	[0.000]	[0.001]
trend break × avg. emissions		0.000	0.000
		(0.000)	(0.000)
		[0.053]	[0.090]
trend break × avg. emissions^2			-0.000
			(0.000)
			[0.158]
	Outcome is asinh($PM_{2.5}$) emissions		
κ_1^p	0.058	0.060	0.060
	(0.043)	(0.042)	(0.043)
	[0.183]	[0.167]	[0.165]
κ_2^p	-0.097	-0.133	-0.146
	(0.048)	(0.051)	(0.068)
	[0.053]	[0.012]	[0.040]
trend break × avg. emissions		-0.004	-0.005
		(0.003)	(0.004)
		[0.197]	[0.249]
trend break × avg. emissions^2			0.000
			(0.000)
			[0.661]
	Outcome is asinh(PM_{10}) emissions		
κ_1^p	0.083	0.084	0.086
	(0.033)	(0.033)	(0.033)
	[0.016]	[0.015]	[0.012]
κ_2^p	-0.117	-0.143	-0.172
	(0.039)	(0.042)	(0.048)
	[0.005]	[0.002]	[0.001]
trend break × avg. emissions		-0.002	-0.003
		(0.001)	(0.002)
		[0.080]	[0.073]
trend break × avg. emissions^2			0.000
			(0.000)
			[0.197]
	Outcome is asinh(NO_x) emissions		
κ_1^p	0.075	0.079	0.080
	(0.039)	(0.038)	(0.039)
	[0.061]	[0.046]	[0.046]
κ_2^p	-0.104	-0.143	-0.157
	(0.050)	(0.045)	(0.079)
	[0.042]	[0.003]	[0.054]
trend break × avg. emissions		-0.001	-0.001
		(0.000)	(0.001)
		[0.002]	[0.294]
trend break × avg. emissions^2			0.000
			(0.000)
			[0.793]
	Outcome is asinh(SO_x) emissions		
κ_1^p	0.006	0.013	0.013
	(0.035)	(0.035)	(0.035)
	[0.875]	[0.715]	[0.705]
κ_2^p	-0.037	-0.110	-0.074
	(0.043)	(0.048)	(0.077)
	[0.393]	[0.026]	[0.345]
trend break × avg. emissions		-0.004	-0.002
		(0.002)	(0.003)
		[0.017]	[0.455]
trend break × avg. emissions^2			-0.000
			(0.000)
			[0.438]

NOTES: Estimates of pre-C&T differential emissions trend (i.e., κ_1^p from equation (1)) and and post-C&T differential emissions trend break (i.e., κ_2^p from equation (1)) for GHG, $PM_{2.5}$, PM_{10}, NO_x, and SO_x across panels. Columns 1 shows benchmark model. Column 2 (3) further interacts post C&T differential trend break with a linear (quadratic) function of sample average annual emissions. All models include facility-specific and year-specific dummy variables. Standard errors clustered at the county-level in parentheses, p-value in brackets.

Table S4: Emissions effect robustness: restricting treatment spillovers

	(1) Benchmark	(2) Nonattainment	(3) Single facilities
	Outcome is asinh(GHG) emissions		
κ_1^p	0.187	-	0.210
	(0.052)	-	(0.053)
	[0.001]	-	[0.000]
κ_2^p	-0.297	-	-0.322
	(0.077)	-	(0.078)
	[0.000]	-	[0.000]
Facilities	316	-	310
Observations	2,054	-	2,029
	Outcome is asinh($PM_{2.5}$) emissions		
κ_1^p	0.058	0.085	0.066
	(0.043)	(0.049)	(0.043)
	[0.183]	[0.092]	[0.137]
κ_2^p	-0.097	-0.119	-0.101
	(0.048)	(0.052)	(0.049)
	[0.053]	[0.029]	[0.046]
Facilities	302	260	299
Observations	1,968	1,729	1,952
	Outcome is asinh(PM_{10}) emissions		
κ_1^p	0.083	0.101	0.091
	(0.033)	(0.034)	(0.033)
	[0.016]	[0.006]	[0.008]
κ_2^p	-0.117	-0.145	-0.121
	(0.039)	(0.054)	(0.040)
	[0.005]	[0.012]	[0.004]
Facilities	302	140	299
Observations	1,968	1,080	1,952
	Outcome is asinh(NO_x) emissions		
κ_1^p	0.075	0.057	0.065
	(0.039)	(0.041)	(0.039)
	[0.061]	[0.173]	[0.101]
κ_2^p	-0.104	-0.090	-0.098
	(0.050)	(0.054)	(0.050)
	[0.042]	[0.102]	[0.060]
Facilities	303	287	300
Observations	1,970	1,879	1,954
	Outcome is asinh(SO_x) emissions		
κ_1^p	0.006	-	0.005
	(0.035)	-	(0.036)
	[0.875]	-	[0.892]
κ_2^p	-0.037	-	-0.036
	(0.043)	-	(0.044)
	[0.393]	-	[0.423]
Facilities	303	-	300
Observations	1,965	-	1,950

NOTES: Estimates of pre-C&T differential emissions trend (i.e., κ_1^p from equation (1)) and and post-C&T differential emissions trend break (i.e., κ_2^p from equation (1)) for GHG, $PM_{2.5}$, PM_{10}, NO_x, and SO_x across panels. Columns 1 shows benchmark model. Column 2 restricts unregulated facilities to those in counties under Clear Air Act nonattainment for pollutant of interest. Nonattainment does not apply for GHG emissions and there were no counties under SO_x nonattainment during our sample period. For NO_x, we use nonattainment in the one-hour ozone standard, for which NO_x is a precursor pollutant. Column 3 restricts unregulated facilities to those whose parent company only operates a single facility. All models include facility-specific and year-specific dummy variables. Standard errors clustered at the county-level in parentheses, p-value in brackets.

Table S5: Correlation between HYSPLIT-driven and ambient pollution exposure

	(1)	(2)	(3)	(4)
	Outcome is ambient asinh(exposure)			
	$PM_{2.5}$	PM_{10}	NO_x	SO_x
HYSPLIT-driven asinh(exposure)	0.860	0.625	0.436	0.231
	(0.154)	(0.137)	(0.148)	(0.207)
	[0.000]	[0.000]	[0.004]	[0.272]
Zip codes	133	160	121	39

NOTES: Linear coefficient from zip code-level regressions of asinh daily HYSPLIT-driven pollution exposure (in $\mu g/m^3/day$) averaged across 2008-2017 on asinh daily pollution exposure from ambient pollution monitors (in $\mu g/m^3/day$) averaged across 2008-2017. We employ a asinh-asinh specification because ambient pollution readings, which capture the average daily instantaneous stock of pollution, are not directly comparable to our exposure measure, which capture average daily pollution flow from C&T-driven emissions. Ambient pollution are assumed to be uniformly distributed within a monitor's zip code. Standard errors clustered at the county-level in parentheses, p-value in brackets.

Table S6: Pollution exposure difference between disadvantaged and other zip codes in 2008

	(1) Disadvantaged	(2) Other	(3) Difference
$PM_{2.5}$	0.256	0.093	0.163
	(0.888)	(0.572)	(0.038)
			[0.000]
PM_{10}	0.322	0.109	0.214
	(1.066)	(0.532)	(0.043)
			[0.000]
NO_x	0.451	0.387	0.064
	(2.842)	(6.856)	(0.243)
			[0.792]
SO_x	0.364	0.091	0.273
	(1.092)	(0.217)	(0.041)
			[0.000]
Zip codes	722	984	1,706

NOTES: Column 1 shows average 2008 pollution exposure ($\mu g/m^3$) across disadvantaged zip codes, with standard deviation in parentheses. Column 2 shows average 2008 pollution exposure ($\mu g/m^3$) across other zip codes, with standard deviation in parentheses. Column 3 shows the average difference in 2008 pollution exposure between disadvantaged and other zip codes, with standard error in parentheses and p-value in brackets. All pollution exposure generated by HYSPLIT from facilities that would eventually be regulated by the GHG C&T program.

Table S7: EJ gap effect robustness: step 1

	(1) Year-specific effects	(2) GHG cutoff: 70%	(3) GHG cutoff: 80%	(4) Hetero in avg. emissions	(5) SUTVA NA	(6) SUTVA Single fac.
			Panel a: $PM_{2.5}$			
β_1^p	0.040	0.025	0.043	0.041	0.048	0.043
	(0.011)	(0.006)	(0.010)	(0.012)	(0.012)	(0.012)
	[0.001]	[0.000]	[0.000]	[0.001]	[0.000]	[0.000]
β_2^p	-0.061	-0.031	-0.063	-0.075	-0.067	-0.064
	(0.019)	(0.008)	(0.019)	(0.021)	(0.021)	(0.020)
	[0.003]	[0.000]	[0.001]	[0.001]	[0.002]	[0.002]
$(\beta_2^p/\beta_1^p) * 100$	-152.583	-125.385	-146.581	-182.096	-141.543	-146.262
Observations	16,416	16,387	16,426	16,416	16,416	16,416
			Panel b: PM_{10}			
β_1^p	0.062	0.038	0.069	0.064	0.074	0.066
	(0.014)	(0.008)	(0.013)	(0.014)	(0.016)	(0.015)
	[0.000]	[0.000]	[0.000]	[0.000]	[0.000]	[0.000]
β_2^p	-0.089	-0.046	-0.093	-0.100	-0.105	-0.091
	(0.027)	(0.009)	(0.026)	(0.028)	(0.030)	(0.028)
	[0.002]	[0.000]	[0.001]	[0.001]	[0.001]	[0.002]
$(\beta_2^p/\beta_1^p) * 100$	-142.447	-121.310	-134.948	-156.155	-141.932	-136.905
Observations	16,416	16,387	16,426	16,416	16,416	16,416
			Panel c: NO_x			
β_1^p	0.079	0.043	0.087	0.079	0.079	0.082
	(0.033)	(0.026)	(0.031)	(0.033)	(0.032)	(0.034)
	[0.019]	[0.108]	[0.006]	[0.021]	[0.018]	[0.018]
β_2^p	-0.132	-0.055	-0.149	-0.142	-0.138	-0.141
	(0.066)	(0.031)	(0.069)	(0.075)	(0.070)	(0.071)
	[0.051]	[0.084]	[0.035]	[0.062]	[0.052]	[0.053]
$(\beta_2^p/\beta_1^p) * 100$	-167.212	-128.157	-170.878	-180.760	-175.096	-172.408
Observations	16,416	16,387	16,426	16,416	16,416	16,416
			Panel d: SO_x			
β_1^p	0.036	0.023	0.037	0.011	-	0.037
	(0.022)	(0.015)	(0.020)	(0.012)	-	(0.023)
	[0.108]	[0.141]	[0.077]	[0.349]	-	[0.108]
β_2^p	-0.103	-0.080	-0.099	-0.114	-	-0.100
	(0.050)	(0.045)	(0.046)	(0.058)	-	(0.049)
	[0.045]	[0.084]	[0.037]	[0.054]	-	[0.047]
$(\beta_2^p/\beta_1^p) * 100$	-284.826	-353.380	-267.896	-1003.707	-	-272.630
Observations	16,416	16,387	16,426	16,416	-	16,416

NOTES: Estimates of the pre-C&T EJ gap trend (i.e., β_1^p from equation (2)), post-C&T EJ gap trend break (i.e., β_2^p from equation (2)), and the percentage change in the EJ gap trend following the introduction of the C&T program (i.e., $\frac{\beta_2^p}{\beta_1^p} * 100$) for $PM_{2.5}$, PM_{10}, NO_x, and SO_x down panels. All models include zip code-specific and year-specific dummy variables. Observations weighted by zip code-level average population during 2008-2012. Column 1 uses year-specific effects to estimate C&T-driven emissions. Columns 2 and 3 restrict facilities to those with sample average GHG emissions below the 70th and 80th percentile, respectively to estimate C&T-driven emissions (see columns 1 and 3 of Table S2). Column 4 uses C&T-driven emissions that allow the C&T differential trend break to vary as a linear function of sample average emissions (see column 2 of Table S3). Column 5 restricts unregulated facilities to those in counties under Clear Air Act nonattainment for pollutant of interest (see column 2 of Table S4). Column 6 restricts unregulated facilities to those whose parent company only operates a single facility (see column 3 of Table S4). Standard errors, in parentheses, cluster ϵ_{it}^p from equation (2) at the county-level but are not adjusted for statistical uncertainty from equation (1). P-value in brackets. Observations apply to all panels.

Table S8: EJ gap effect robustness: steps 2 and 3

	(1) Slower decay	(2) Faster decay	(3) Lower boundary	(4) Higher boundary	(5) Spatial corr. err.	(6) Pollution corr. err.
			Panel a: $PM_{2.5}$			
β_1^p	0.043	0.041	0.037	0.043	0.042	0.042
	(0.011)	(0.011)	(0.010)	(0.011)	(0.004)	(0.006)
	[0.000]	[0.000]	[0.001]	[0.000]	[0.000]	[0.000]
β_2^p	-0.064	-0.062	-0.055	-0.064	-0.063	-0.063
	(0.020)	(0.020)	(0.019)	(0.020)	(0.009)	(0.010)
	[0.002]	[0.003]	[0.007]	[0.002]	[0.000]	[0.000]
$(\beta_2^p/\beta_1^p) * 100$	-149.007	-150.533	-148.764	-149.992	-149.699	-149.699
			Panel b: PM_{10}			
β_1^p	0.066	0.063	0.057	0.066	0.065	0.065
	(0.015)	(0.014)	(0.013)	(0.014)	(0.006)	(0.008)
	[0.000]	[0.000]	[0.000]	[0.000]	[0.000]	[0.000]
β_2^p	-0.092	-0.089	-0.079	-0.092	-0.090	-0.090
	(0.027)	(0.027)	(0.027)	(0.027)	(0.011)	(0.013)
	[0.001]	[0.002]	[0.005]	[0.001]	[0.000]	[0.000]
$(\beta_2^p/\beta_1^p) * 100$	-139.150	-140.448	-137.785	-140.161	-139.739	-139.739
			Panel c: NO_x			
β_1^p	0.089	0.081	0.083	0.085	0.085	0.085
	(0.036)	(0.034)	(0.035)	(0.035)	(0.039)	(0.021)
	[0.018]	[0.020]	[0.020]	[0.018]	[0.030]	[0.000]
β_2^p	-0.148	-0.139	-0.140	-0.144	-0.143	-0.143
	(0.073)	(0.073)	(0.073)	(0.073)	(0.050)	(0.033)
	[0.048]	[0.063]	[0.060]	[0.054]	[0.004]	[0.000]
$(\beta_2^p/\beta_1^p) * 100$	-166.117	-170.804	-168.674	-168.261	-168.282	-168.282
			Panel d: SO_x			
β_1^p	0.037	0.037	0.030	0.038	0.037	0.037
	(0.023)	(0.022)	(0.019)	(0.023)	(0.007)	(0.006)
	[0.109]	[0.107]	[0.133]	[0.103]	[0.000]	[0.000]
β_2^p	-0.102	-0.100	-0.087	-0.102	-0.101	-0.101
	(0.050)	(0.049)	(0.044)	(0.050)	(0.012)	(0.010)
	[0.047]	[0.047]	[0.053]	[0.045]	[0.000]	[0.000]
$(\beta_2^p/\beta_1^p) * 100$	-271.967	-272.688	-295.166	-270.107	-272.291	-272.291
Observations	16,416	16,416	16,359	16,430	16,417	16,417

NOTES: Estimates of the pre-C&T EJ gap trend (i.e., β_1^p from equation (2)), post-C&T EJ gap trend break (i.e., β_2^p from equation (2)), and the percentage change in the EJ gap trend following the introduction of the C&T program (i.e., $\frac{\beta_2^p}{\beta_1^p} * 100$) for $PM_{2.5}$, PM_{10}, NO_x, and SO_x down panels. All models include zip code-specific and year-specific dummy variables. Observations weighted by zip code-level average population during 2008-2012. Column 1 applies a slower pollution decay to HYSPLIT pollution trajectories (i.e., 10% larger half-life parameter). Column 2 applies a faster pollution decay to HYSPLIT pollution trajectories (i.e., 10% smaller half-life parameter). Column 3 applies a lower planetary boundary layer set at 0.5 km. Column 4 applies a higher planetary boundary layer set at 2 km. Column 5 adjusts standard errors for spatial (500 km uniform kernel) and serial correlation (5 years). Column 6 adjusts standard errors allowing correlation across pollutants using a Seemingly Unrelated Regression (SUR) procedure. Standard errors, in parentheses, cluster ϵ_{it}^p from equation (2) at the county-level but are not adjusted for statistical uncertainty from equation (1). P-value in brackets. Observations apply to all panels.

Table S9: EJ gap effect robustness: asinh exposure

	(1)	(2)	(3)	(4)
	Outcome is (asinh) exposure			
	$PM_{2.5}$	PM_{10}	NO_x	SO_x
β_1^p	0.027	0.037	0.032	0.017
	(0.013)	(0.014)	(0.021)	(0.017)
	[0.045]	[0.009]	[0.137]	[0.336]
β_2^p	-0.032	-0.042	-0.038	-0.051
	(0.014)	(0.015)	(0.023)	(0.030)
	[0.026]	[0.009]	[0.102]	[0.095]
$\beta_1^p + \beta_2^p$	-0.006	-0.004	-0.005	-0.034
	(0.005)	(0.007)	(0.008)	(0.015)
	[0.302]	[0.551]	[0.487]	[0.029]
Zip codes	1649	1649	1649	1649
Counties	58	58	58	58
Observations	16,416	16,416	16,416	16,416

NOTES: Estimates of the pre-C&T EJ gap trend (i.e., β_1^p from equation (2)), the post-C&T EJ gap trend break (i.e., β_2^p from equation (2)), and the post-C&T EJ gap trend (i.e, $\beta_1^p + \beta_2^p$) for asinh($PM_{2.5}$), asinh(PM_{10}), asinh(NO_x), and asinh(SO_x), across columns. All models include zip code-specific and year-specific dummy variables. Observations weighted by zip code-level average population during 2008-2012. Parentheses indicate standard errors that account for statistical uncertainty in C&T predicted emissions (μ_{it}^p from equation (1) via the bootstrap procedure in Appendix A.1) and county-level heterogeneity in EJ gap effects of arbitrary form (ϵ_{it}^p from equation (2)). P-value in brackets.

Table S10: EJ gap effect robustness: total $PM_{2.5}$ exposure using InMAP

	(1) Primary $PM_{2.5}$	(2) Total $PM_{2.5}$
β_1^p	0.002	0.003
	(0.001)	(0.001)
	[0.001]	[0.001]
β_2^p	-0.003	-0.004
	(0.001)	(0.001)
	[0.000]	[0.000]
$\beta_1^p + \beta_2^p$	-0.001	-0.002
	(0.000)	(0.001)
	[0.004]	[0.001]
$(\beta_2^p/\beta_1^p) * 100$	-150.559	-172.948
	(16.261)	(16.415)
	[0.000]	[0.000]
Zip codes	1648	1648
Counties	58	58
Observations	16,480	16,480

NOTES: Estimates of the pre-C&T EJ gap trend (i.e., β_1^p from equation (2)), the post-C&T EJ gap trend break (i.e., β_2^p from equation (2)), the post-C&T EJ gap trend (i.e, $\beta_1^p + \beta_2^p$), and the percentage change in the EJ gap trend following the introduction of the C&T program (i.e., $\frac{\beta_2^p}{\beta_1^p} * 100$) for InMAP-modeled primary $PM_{2.5}$ exposure (column 1) and for InMAP-modeled total (i.e., primary and secondary) $PM_{2.5}$ exposure (column 2). InMAP employs dispersal patterns for 2005 and not for the 2008-2017 sample period. All models include zip code-specific and year-specific dummy variables. Observations weighted by zip code-level average population during 2008-2012. Standard errors, in parentheses, cluster ϵ_{it}^p from equation (2) at the county-level but are not adjusted for statistical uncertainty from equation (1). P-value in brackets.

Table S11: Importance of modeling pollution dispersal

	(1) Facility zip code	(2) 1.6 km circle	(3) 4 km circle	(4) 10 km circle
		Panel a: $PM_{2.5}$		
β_1^p	0.052	-0.017	-0.075	-0.140
	(0.036)	(0.026)	(0.040)	(0.079)
	[0.157]	[0.527]	[0.075]	[0.084]
β_2^p	-0.076	-0.003	0.067	0.132
	(0.049)	(0.023)	(0.036)	(0.072)
	[0.134]	[0.912]	[0.075]	[0.076]
Observations	785	1,831	3,573	7,545
		Panel b: PM_{10}		
β_1^p	0.105	0.020	-0.069	-0.143
	(0.070)	(0.030)	(0.047)	(0.089)
	[0.142]	[0.509]	[0.155]	[0.116]
β_2^p	-0.142	-0.049	0.059	0.137
	(0.091)	(0.036)	(0.055)	(0.095)
	[0.132]	[0.177]	[0.294]	[0.157]
Observations	785	1,831	3,573	7,545
		Panel c: NO_x		
β_1^p	0.163	-0.120	-0.292	-0.417
	(0.188)	(0.110)	(0.096)	(0.175)
	[0.391]	[0.285]	[0.005]	[0.022]
β_2^p	-0.213	0.103	0.311	0.480
	(0.247)	(0.132)	(0.110)	(0.179)
	[0.396]	[0.442]	[0.008]	[0.011]
Observations	785	1,831	3,573	7,545
		Panel d: SO_x		
β_1^p	0.001	-0.156	-0.273	-0.433
	(0.004)	(0.122)	(0.183)	(0.250)
	[0.688]	[0.210]	[0.145]	[0.091]
β_2^p	-0.014	-0.007	0.128	0.253
	(0.009)	(0.030)	(0.103)	(0.143)
	[0.125]	[0.813]	[0.223]	[0.085]
Observations	783	1,823	3,553	7,535

NOTES: Estimates of the pre-C&T EJ gap trend (i.e., β_1^p from equation (2)) and the post-C&T EJ gap trend break (i.e., β_2^p from equation (2)) for $PM_{2.5}$, PM_{10}, NO_x, and SO_x down panels. All models include zip code-specific and year-specific dummy variables. Observations weighted by zip code-level average population during 2008-2012. Column 1 assigns pollution exposure to only the zip code of the emitting facility. Columns 2-4 assign pollution exposure to zip codes with centroid within a 1.6, 4 km and 10 km circle of emitting facility, respectively. Standard errors in parentheses cluster ϵ_{it}^p from equation (2) at the county-level but are not adjusted for statistical uncertainty from equation (1). P-value in brackets.